การผลิตเอทิลีนจากเอทานอลบนตัวเร่งปฏิกิริยาชนิดซีโอไลต์ ZSM-5 ชนิดดัดแปลง

นางสาว อุณาโลม เวทย์วัฒนะ
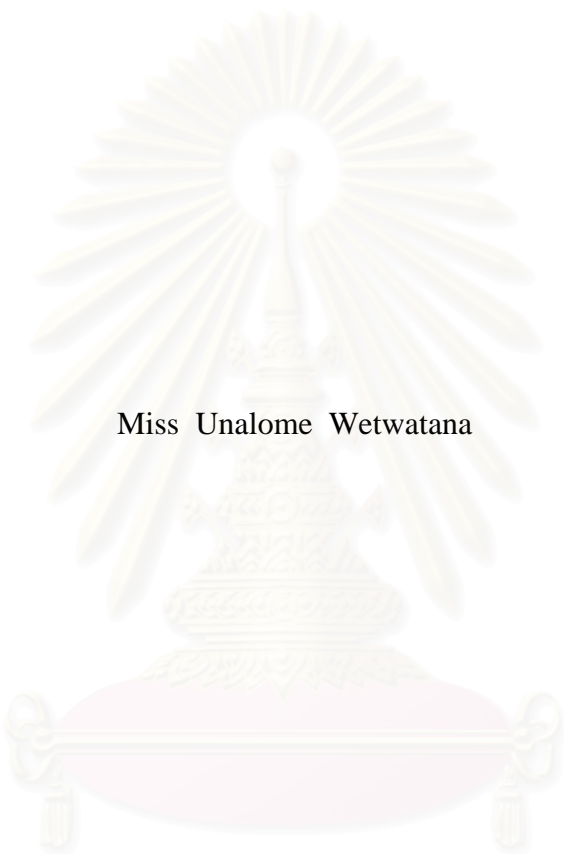
PRODUCTION OF ETHYLENE FROM ETHANOL ON MODIFIED
ZSM-5 ZEOLITES

Miss Unalome Wetwatana

Thesis Title	Production of Ethylene from Ethanol on Modified ZSM-5 zeolite
By	Miss Unalome Wetwatana
Field of Study	Chemical Engineering
Thesis Advisor	Suphot Phatanasri, D.Eng.
Thesis Co-adviser	Professor Piyasan Praserthdam, Dr.Ing.

_____

Accepted by the Faculty of Engineering, Chulalongkorn University in Partial Fulfillment of the Requirements for the Master's Degree

………..……………..……….Dean of Faculty of Engineering

(Professor Somsak Panyakeow, D.Eng)

Thesis Committee

……………………………………….Chairman

(Montree Wongsri, D.Sc.)

……………………………………….Thesis Advisor

(Suphot Phatanasri, D.Eng.)

……………………………………….Thesis Co-advisor

(Professor Piyasan Praserthdam, Dr.Ing.)

……………………………………….Member

(Assistant Professor M.L. Supakanok Thongyai, Ph.D.)

……………………………………….Member

(Assistant Professor Seeroong Prichanont, Ph.D.)

อุณาโลม เวทย์วัฒนะ : การผลิตเอทิลีนจากเอทานอลบนตัวเร่งปฏิกิริยาชนิดซีโอไลต์ ZSM-5 ชนิดดัดแปลง (PRODUCTION OF ETHYLENE FROM ETHANOL ON MODIFIED ZSM-5 ZEOLITES) อ. ที่ปรึกษา : อ.ดร.สุพจน์ พัฒนะศรี, อ.ที่ปรึกษาร่วม : ศ.ดร.ปิยะสาร ประเสริฐธรรม, 62 หน้า

งานวิจัยนี้มีวัตถุประสงค์เพื่อทำการศึกษาการเปลี่ยนเอทานอลด้วยปฏิกิริยาขจัดน้ำ หรือ ดี ไฮเดรชัน เพื่อให้ได้เอทิลีนบนตัวเร่งปฏิกิริยาซีโอไลต์ชนิด ZSM-5 และ ZSM-5 ชนิดดัดแปลง โดยเลือกใช้โลหะเหล็ก (Fe) เตรียมตัวเร่งปฏิกิริยา ZSM-5 ชนิดดัดแปลงด้วยวิธีการแลกเปลี่ยนอิ ออน และวิธีการตกผลึก พบว่า อุณหภูมิ ปริมาณโลหะเหล็ก และความเร็วเชิงสเปซที่เหมาะสม ต่อการเปลี่ยนเอทานอลบนตัวเร่งปฏิกิริยาซีโอไลต์ชนิด ZSM-5 คือ 600 องศาเซลเซียส ร้อยละ 5 ของโลหะเหล็กโดยน้ำหนักบนตัวเร่งปฏิกิริยา และ 2000 ต่อชั่วโมงตามลำดับ ผลิตภัณฑ์ ไฮโดรคาร์บอนหลักที่ได้ คือ เอทิลีน และ ไดเอทิลอีเทอร์ ในภาวะนี้การเลือกเกิดเป็นเอทิลีนจะ มีค่าเป็น 83% ในขณะที่การเปลี่ยนเอทานอลเป็น 95% พบว่าการเกิดเอทิลีนอาจจะเกิดผ่านได เอทิลอีเทอร์ การเปลี่ยนความเร็วเชิงสเปซของเอทานอลจาก 6000 ต่อชั่วโมง เป็น 2000 ต่อชั่ว โมง ทำให้ปริมาณการเลือกเกิดของเอทิลีนเพิ่มขึ้น เมื่อเปรียบเทียบตัวเร่งปฏิกิริยา 5%Fe-ZSM-5 ที่เตรียมโดยวิธีการแลกเปลี่ยนอิออน และวิธีการตกผลึก พบว่าตัวเร่งปฏิกิริยา 5%Fe-ZSM-5 ที่ เตรียมโดยวิธีการแลกเปลี่ยนอิออน มีการเลือกเกิดเป็นเอทิลีนสูงกว่าตัวเร่งปฏิกิริยา 5%Fe-ZSM-5 ที่เตรียมโดยวิธีการตกผลึก ซึ่งเป็นผลมาจากโครงสร้างของตัวเร่งปฏิกิริยาที่แตกต่างกันส่งผลต่อ ประสิทธิภาพในการทำงานของตัวเร่งปฏิกิริยา

ภาควิชา.............วิศวกรรมเคมี.............. ลายมือชื่อนิสิต..
สาขาวิชา............วิศวกรรมเคมี.............. ลายมือชื่ออาจารย์ที่ปรึกษา...........................
ปีการศึกษา.........2545........................ ลายมือชื่ออาจารย์ที่ปรึกษาร่วม......................

 # # 4370628021: MAJOR CHEMICAL ENGINEERING
KEY WORD: ZSM-5 / ETHANOL / DEHYDRATION

UNALOME WETWATANA: PRODUCTION OF ETHYLENE FROM ETHANOL ON MODIFIED ZSM-5 ZEOLITES. THESIS ADVISOR: SUPHOT PHATANASRI, Dr. Eng, THESIS CO-ADVISOR: PROF. PIYASAN PRASERTHDAM, Dr.Ing. 62 pp.

Dehydration of Ethanol to Ethylene on modified ZSM-5 zeolites. Containing a iron metal was investigated in this research. The catalyst were prepared by ion-exchange method and rapid crystallization method. It has been found that the appropriate reaction temperature, the percentage of Fe loading and GHSV over Fe-ZSM-5 catalyst were 600°C, 5% by weight and 2000 h^{-1}, respectively. The main hydrocarbon products from this reaction were ethylene and diethyl ether. The selectivity to ethylene was 83% at 95% ethanol conversion. It was suggested that the formation of ethylene possible proceeded via diethyl ether intermediate. With the effect of space velocity of ethanol was decreased from 6000 h^{-1} to 2000 h^{-1}, resulted increase selectivity to ethylene. Comparation between 5%Fe-ZSM-5 prepared by ion-exchange method and rapid crystallization method. It has been found that 5%Fe-ZSM-5 prepared by ion-exchange method resulted in the higher selective than 5%Fe-ZSM-5 prepared by rapid crystallization method.

Department……………………..   Student's signature……………………………..

Field of study…………………..   Advisor's signature……………………………..

Academic year………………....   Co-advisor's signature…………………………..

ACKNOWLEDGEMENTS

CONTENT

LIST OF TABLES

LIST OF FIGURES

CHAPTER I
INTRODUCTION

Ethanol is currently produced by hydration of ethylene which is derived mainly by steam-cracking of petroleum or natural gas feed stocks. Ethanol can also be obtained by the anaerobic fermentation of sugars (mostly glucose) which in turn are the products of (acid or enzymatic) hydrolysis of cellulosic compounds. [N.P. Cheremisinoff, D.L. Klass (1987)]. These compounds can be "extracted" from biomass, particularly wood materials. Due to today's low cost of petroleum ethanol and the relative high production cost of fermentation ethanol, the competitiveness of the latter is regularly the subject of discussion.

Ethanol present at low concentration in a fermentation broth which also contains some leftover glucose as well as other fermentation residues, is totally converted into ethylene over ZSM-5 catalyst. A rapid economical evaluation shows that ethylene produced by B.E.T.E. (bio-ethanol-to-ethylene) process has a production cost 10% to 40% higher than petroleum ethylene. However, a more promising figure can be envisaged with a better integrated process working with cheaper raw materials.

Gasoline can be produced from ethanol by catalytic conversion over ZSM-5 type zeolite. In the latter process, a concentration of ethanol of at least 60 vol% is necessary. Thus, according to the today's state of art, two steps are needed to produce ethylene or gasoline (the first step being the ethanol distillation from the fermentation broth).

In our laboratory, zeolite catalysts which allow the production of practically pure ethylene from aqueous ethanol (concentration = 20%wt) have been developed. This also means that ethylene can be produced directly from ethanol fermentation broth in a one-step process. The latest version of these catalysts, a 5%Fe-ZSM-5 zeolite, can catalyse the reaction at temperature 600°c and under atmospheric pressure.

However should this route become of industrial significance it could lead to the paradox that in some parts of the world ethanol would be dehydrated to ethylene while elsewhere ethylene would be hydrated to produce ethanol.

1.1 The objective of this study

1. To study the preparation method of iron containing ZSM-5 zeolite catalysts.

2. To characterize the prepared catalysts.

3. To investigate the performance of the prepared catalysts on ethanol dehydration.

4. To find operating optimum condition on dehydration of ethanol.

1.2 The scope of this study

1. Study of method to introduce iron ZSM-5 zeolite catalyst either by ion-exchange and rapid crystallization method.

2. Study the characterization of the prepared catalysts by following methods.

- Analyzing structure of catalysts by X-ray diffraction (XRD)

- Analyzing amount of iron of catalysts by X-ray fluorescence (XRF)

- Analyzing shape and size of crystallites by scanning electron microscopy (SEM)

- Analyzing surface areas of catalysts by Brunauer-Emmett-Teller (BET) Surface Areas Measurement.

- Analyzing the acidity of catalysts by Temperature Programmed Desorption of Ammonia (NH$_3$-TPD)

3. Investigate the performance of the prepared catalysts on the dehydration of ethanol under the following condition.

- Atmospheric pressure

- Reaction temperature 400-600 °C

- Space velocity 2000-6000 h^{-1}

- Reactant feed 20Wt% ethanol

The reaction products were analyzed by Gas Chromatography.

CHAPTER II
LITERATURE REVIEWS

In this section, special attention of related papers devoted directly to the dehydration of ethanol over catalysts. However, the other points which related to this reaction are also mentioned so that all information can contribute and lead to some interesting subjects concerned in this thesis.

Winfield *et al.* (1960), studies about acid catalyzed ethanol dehydration to ethylene. The selective conversion of ethanol to ethylene in mildly acidic homogeneous solution was first detected by Bondt over 200 years ago. The heterogeneous catalysis of this reaction has been practice before the turn of the 20th century on the industrial scale by passing ethanol vapors at atmospheric pressure over γ-Al_2O_3 or a supported acid catalyst at 588-668 K. Ethylene is typically assumed to be produced via a simultaneous parallel-consecutive involving direct ethanol conversion as well as by the consecutive reaction

$$2C_2H_5OH \longrightarrow C_2H_5OC_2H_5 \longrightarrow 2C_2H_4 + 2H_2O$$

At low temperatures (<503 K), diethyl ether is produced in significant quantities, while, at a high temperatures (>573 K), ethylene is the dominant product. Alcohol dehydrogenation to produce acetaldehyde can also occur as a side reaction at the higher temperatures, depending upon the impurities in Al_2O_3.

Tsao and Reilly (1978), proposed process is based on three well-known industrial reactions. Hydrous ethanol feed is subjected to catalytic dehydration to form ethylene

$$C_2H_5OH \longrightarrow C_2H_4 + H_2O$$
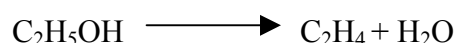
This product stream is cooled and dimerized to n-butene

$$2C_2H_4 \longrightarrow n\text{-}C_4H_8$$
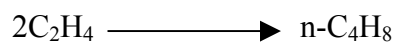
the n-butene effluent is next converted by skeletal isomerization to isobutylene

$$n\text{-}C_4H_8 \longleftrightarrow CH_3-\underset{\underset{}{|}}{\overset{\overset{CH_3}{|}}{C}}=CH_2$$

which is compressed and combined with anhydrous ethanol in an etherification reactor/catalytic distillation unit to produce ETBE

$$C_2H_5OH + CH_3-\overset{\overset{CH_3}{|}}{C}=CH_2 \longleftrightarrow CH_3-\overset{\overset{CH_3}{|}}{\underset{\underset{CH_3}{|}}{C}}-O-C_2H_5$$
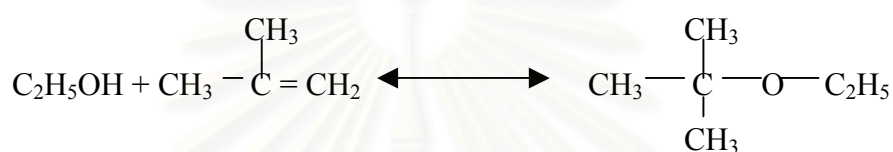
Thus, by summing equation (1)-(4), the overall transformation is

$$3\ C_2H_5OH \longleftrightarrow CH_3-\overset{\overset{CH_3}{|}}{\underset{\underset{CH_3}{|}}{C}}-O-C_2H_5$$

It may, of couse, be possible to design catalysts that may combine some of above processing steps.

Chen *et al.* (1983), discussed the effluence of small quantities of water in the ethanol feed on the observed reaction kinetics under differential reactor conditions for the parallel reactions simultaneously forming ethylene and diethyl ether. If water in amounts greater than 5 Vol% can be incorporated in the ethanol feed, the feed stock cost reduces significantly

Hegde S.G. *et al.* (1983), observed the NH_3-TPD profiles of various metal ion ZSM-5 catalysts showed three peaks at 150-250, 250-350 and 350-450 °C corresponding to the desorption of NH_3 from weak, medium and strong acid sites, respectively. The metal ion-modified catalysts showed more medium and weak acidic sites than H-ZSM-5 catalysts. The total acidity of the catalysts followed the order Mn-ZSM-5<Cu-ZSM-5<Fe-ZSM-5<Pb-ZSM-5<H-ZSM-5<Co-ZSM-5<La-ZSM-5

Jingfa *et al.* (1988), studied the surface reaction mechanism using infrared spectroscopy and concluded that ethanol may be converted into either ethylene or diethyl ether via an ethyloxonium intermediate. Much of more recent work on this reaction has been done by Le Van Mao and co-workers in their development of the biomass-ethanol-to-ethylene (BETE) process based on ZSM-5 catalysts modified with agents such as trifluoromethanesulfonic acid (TFA), Zn-Mn, La/Ce cations and asbestos

Raymond Le Van Mao *et al.*(1989), studied about the bio-ethanol-to-ethylene (B.E.T.E.) process reported that ethanol present at low concentration in a fermentation broth which also contains some leftover glucose as well as other fermentation residues, is totally converted into ethylene over a solid superacidic catalyst. Trifluoromethanesulfonic acid bound to the silica rich surface of the acidic ZSM-5 zeolite is thermally stable up to 300 °C and can catalyse the reaction with nearly complete conversion at a temperature as low as 170 °C. Below 200 °C, the catalyst is extreamly stable even in the presence of the amount of water found in the feed. A rapid economical evaluation shows that ethylene produced by the B.E.T.E. (bio-ethanol-to-ethylene) process has a production cost 10% to 40% higher than petroleum ethylene.

Moser *et al.* (1989), examined the conversion of an aqueous ethanol solution (10 Wt% ethanol) over H-ZSM-5 with Si/Al ratios from 30-15000 at reaction temperatures between 573 and 773 K. Although products such as diethyl ether, propene and other hydrocarbons were also detected, the reactions forming these byproducts were neglected and the effect of the Si/Al ratio only on the rate of ethylene formation was investigated.

Valyon J. *et al.* (1994), reported preparation procedures of Fe-ZSM-5 catalysts. Catalysts were made from the ammonium or sodium forms of the parent zeolite with a nominal framework Si/Al ratio of 33, supplied by Catal Ltd, (Sheffield, England). The framework Si/Al ratio was determined by Si MAS NMR to be 34±2, using a Bruker spectrometer operating at 500 MHz and a spinning speed of 2 kHz.

Fe-ZSM-5 catalysts have been prepared by four different methods: exchange from aqueous solution, exchange from methanolic solution, exchange by the special technique reported by FH, and exchange in the solid state. Aqueous ion exchange was carried out in a single exchange step at pH 5-6, with solutions of various concentrations (10^{-2}, 10^{-3} mol L^{-1}) of iron (III) nitrate nonahydrate (Aldrich Chemical, > 99.99 % pure). The sample (2 g) was stirred at room temperature, and argon was bubbled through approximately 150 mL of the solution at a flow rate of 5 L/h. Because iron oxy-hydroxide species present in aqueous solution are thought to be inimical to exchange (see below), samples were also prepared by ion exchange in methanol solution. Iron(III) nitrate was dissolved in absolute methanol and then dried with water-free calcium sulfate to remove the water of crystallization. The solution was filtered and mixed with the dried zeolite (20 g L^{-1}). To exclude water vapor from the exchange vessel, dry nitrogen was bubbled through the slurry, which was also irradiated in a 360 W ultrasonic bath. The FH approach is to carry out exchange from Fe(II) rather than Fe(III), using a glass sinter to prevent the access of oxy-hydroxide species to the zeolite. Fe(II) oxalate is used, since the oxalate ion is more easily oxidized by molecular oxygen to CO_2 than is aqueous Fe(II) to Fe(III). Again, argon has been bubbled through the solutions at a rate of 5 L/h and the solution was stirred over a period of 24 h. Iron(II) oxalate (1 g) was slurried in water with 2 g of the zeolite. Samples have been prepared from both sodium and proton forms of the zeolite to test for any influence of the cations present on the stability of the exchanged catalysts. Attempts to prepare solid-state-exchanged samples involved grinding the zeolite with the iron salt under nitrogen in a glovebox (see Table 1) followed by heat treatment before use, as described below. Iron(II) chloride, 0.126 g (Avocado, 99% purity), or Iron (II) carbonate, 0.073 g (ABCR), and 2 g of ZSM-5 were ground together in an agate mortar for about an hour.

Ramaswamy *et al.* (1996), have investigated the structures and acidity of zeolites and the isomorphously substituted zeolites containing different framework atoms, used infrared spectroscopy (IR) and temperature programmed desorption (TPD) of adsorbed NH_3 to study the acidity of several isomorphously substituted M-ZSM-5 with the increased acid strength: Si-(OH)<

B-(OH)-Si << Fe-(OH)-Si < Ga-(OH)-Si < Al-(OH)-Si. For design and characterization of zeolites, and understanding of their catalytical mechanisms, it is desired to get the insight into the detailed structural information. However, X-ray analysis and even more sensitive neutron scattering techniques cannot distinguish between Si and Al or other metal cations in these materials, and these needed information could not be obtained directly from experiments. Thus it is necessary to resort other methods to aquire the information.

Jarvelin *et al* (1996), reported that the commercial production of fuel oxygenate ethers, such as methyl tert-butyl ether (MTBE) and ethyl tert-butyl ether (ETBE), has increased dramatically over the past decade. The isobutylene required for MTBE or ETBE synthesis is available from different sources, e.g., as a by product from steam cracking, fluidized catalytic cracking (FCC), or field butane dehydrogenation and in a variety of grades with weight fractions between 12 and 40%.

Feng X. *et al.* (1997), studied about characterization of the zeolite surface and of the iron spatial distribution. For metal-exchanged zeolites it is always important to have information in the extent to which the metal may be concentrated at or near the external surface. This is particularly important for iron-containing materials because of the complexity of that metal's aqueous chemistry. We have used both transmission electron microscopy combined with elemental analysis and XPS to study the distribution of iron-containing species through our samples.

Cory B. Phillips *et al.* (1997), observed the production of ethylene from hydrous ethanol on H-ZSM-5 under mild conditions. Due to the dramatic rise in the use of ethers as fuel oxygenates, an alternative process for the production of ethyl tert-butyl ether (ETBE) based solely on biomass-derive ethanol feedstock is proposed. The first step in this process is ethanol dehydration on H-ZSM-5 to produce ethylene. Hydrous ethanol is a particularly attractive feedstock for this step since the production of anhydrous ethanol is very energy/cost intensive. In fact, the presence of water in the ethanol feed enhances the steady-state activity and selectivity of H-ZSM-5 catalysts.

Reaction kinetic data were collected in a microreactor at temperatures between 413 and 493 K, at ethanol partial pressures of less than 0.7 atm, and at water feed molar ratios of less than 0.25. A sharp initial decline in catalyst activity observed within a few minutes on stream was attributed to the formation of "low-temperature coke" from ethylene oligomerization. Deactivatation occurred at a much slower rate after 100 min on stream, allowing near-steady-state data to be collected. Water in the ethanol feed enhanced the steady-state catalytic activity and ethylene selectivity by moderating the acidity of the catalytic sites, resulting in less extensive deactivation due to coking.

Richard Joyner *et al.* (1999), studied about preparation, characterization and performance of Fe-ZSM-5 catalysts. A number of iron-ZSM-5 catalysts have been prepared and characterized by X-ray absorption spectroscopy using fluorescence detection, electron spectroscopy, temperature programmed reduction, infrared spectroscopy and electron microscopy. Iron has been introduced by aqueous exchange, by a novel method recently proposed by Feng and Hall, by exchange from a rigorously dried methanolic solution accompanied by agitation with ultrasound, and by a method intended to promote solid-state exchange. The degree of interaction with the zeolite framework has been probed by examining the effect on the zeolite proton OH band in the infrared spectrum. Less than 30% of the protons were exchanged from aqueous solution, but almost 80% exchange was achieved using ultrasound, as well as by the method reported by FH. Initially, both methods exhibited mainly isolated metal ions; however, calcination of the samples prepared according to FH exhibited rather large oxide clusters. After aqueous exchange and actication, most of iron is present in the form of small oxygen-containing nanoclusters within the zeolite matrix, with EXAFS measurements indicating an average composition of Fe_4O_4, although electron microscopy identifies some larger particles at the external surface of the zeolite. Depending on the preparation methods, isolated cationic species within the zeolite matrix were also found. The small Fe_4O_4 type clusters cannot be reduced to the metallic state, even by hydrogen at 1100 K, although interconversion between Fe(II) and Fe(III) is facile. When the zeolite was exposed to nitric oxide, stretching vibrations corresponding to adsorption on the different iron species present could be identified by infrared

spectroscopy. It is proposed that the ultrastable iron-oxygen nanoclusters have structures similar either to the iron-sulfur compounds ferredoxin II of desulfovibrio Gigas or to the cubanes of high-potential iron protein (HIPIP). Reactivity of these Fe-ZSM-5 materials in the selectivity catalytic reduction of NO_x by propene in oxygen/helium differs significantly, depending irreversibly on whether they are initially activated in oxygen or in an inert atmosphere. Correlations between catalytic activity and the infrared spectroscopy results for adsorbed NO indicate that the nanoclusters are more active (per iron atom) in the SCR reaction than the isolated cations.

N.Srinivas *et al.* (2002) studied about shape-selective synthesis of collidines over modified zeolites. The number of water molecules per unit cell as estimated from the TG weight loss of the catalyst between 150 and 250 °C, showed that the Pb-, Mn- and La-ZSM-5 samples adsorbed a larger number of water molecules than the H-ZSM-5 sample, while the Fe-, Co- and Cu-ZSM-5 samples adsorbed a smaller number.

S.P. Yuan and J.G. Wang *et al.* (2002) investigated Bronsted acidity of isomorphously substituted ZSM-5 by B, Al, Ga and Fe density functional. The Bronsted acidity of isomorphously substituted ZSM-5 by B, Al, Ga and Fe has been studied at the B3LYP level of density functional theory. On the basis of the calculated proton affinity, natural charge on the acidic proton, and the adsorption energy of NH_3, the Bronsted acidity increases in the order: B-(OH)-Si < Fe-(OH)-Si < Ga-(OH)-Si < Al-(OH)-Si, in agreement with the experiment. In both Al and Ga modified clusters, the adsorbed NH_3 becomes ammonium (NH_4^+) stabilized by two N-H..O hydrogen bonds, while the physisorbed NH_3 is stabilized by one N..H-O hydrogen bond in Fe and B substituted clusters. It is also found that NH_3 adsorption changes the B coordination sphere.

CHAPTER III
THEORY

3.1 Zeolite

The name of "zeolite" comes from the Greek words zeo (to boil) and lithos (stone). The classical definition of a zeolite is a crystalline, porous aluminosilicate. However, some relatively recent discoveries of materials virtually identical to the classical zeolite,but consisting of oxide structures with elements other than silicon and aluminum have stretched the definition. Most researchers now include virtually all types of porous oxide structures that have well-defined pore structures due to a high degree of crystallinity in their definition of the zeolite.

In these crystalline materials we call zeolites, the metal atoms (classically, silicon or aluminum) are surrounded by four oxygen anions to form an approximate tetrahedron consisting of a metal cation at the center and oxygen anions at the four apexes. The tetrahedra metals are called T-atoms for short, and these tetrahedra then stack in beautiful, regular arrays such that channels form. The possible ways for the stacking to occur is virtually limitless, and hundreds of unique structures are known. Graphical depictions of several representative types are given under "Representative Structures".

The zeolitic channels (or pores) are microscopically small, and in fact, have molecular size dimensions such that they are often termed "molecular sieves". The size and shape of the channels have extraordinary effects on the properties of these materials for adsorption processes, and this property leads to their use in separation processes. Molecules can be separated via shape and size effects related to their possible orientation in the pore, or by differences in strength of adsorption.

Since silicon typically exits in a 4+ oxidation state, the silicon-oxygen tetrahedra are electrically neutral. However, in zeolites, aluminum typically

exists in the 3+ oxidation state so that aluminum-oxygen tetrahedra form centers that are electrically deficient one electron. Thus, zeolite frameworks are typically anionic, and charge-compensating cations populate the pores to maintain electrical neutrality. These cations can participate in ion-exchange processes, and this yields some important properties for zeolites. When charge-compensating cations are "soft" cations such as sodium, zeolites are excellent water softeners because they can pick up the "hard" magnesium and calcium cations in water leaving behind the soft cations. When the zeolitic cations are protons, the zeolite becomes a strong solid acid. Such solid acids form the foundations of zeolite catalysis applications including the important fluidized bed cat-cracking refinery process. Other types of reactive metal cations can also populate the pores to form catalytic materials with unique properties. Thus, zeolites are also commonly used in catalytic operations and catalysis which zeolites is often called "shape-selective catalysis".

3.2 Structure of Zeolite

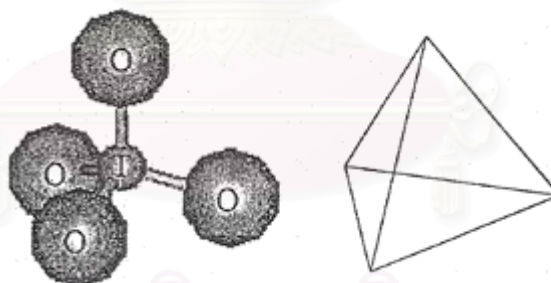**Figure 3.1** TO_4 tetrahedra (T = Si or Al) [Halgeri and Das (1999)]

Zeolites are porous, crystalline aluminosilicate that develop uniform pore structure having minimum channel diameter of 0.3-0.1 nm. This size depens primarily upon the type of zeolite. Zeolites provide high activity and unusual selectivity in a variety of acid-catalyzed reactions. Most of the reactions are caused by the acidic nature of zeolites.

The structure of zeolite consists of a three-dimensional framework of SiO_4 or AlO_4 tetrahedra, each of which contains a silicon or aluminum atom in the center (Figure 3.1) [Halgeri and Das (1999)]. The oxygen atoms are shared between adjoining tetrahedra, which can be present in various ratios and arranged in a variety of way. The framework thus obtained contains pores, channels, and cages, or interconnected voids.

A secondary building unit (SBU) consists of selected geometric groupings of those tetrahedral. There are sixteen such building units, which can be used to describe all of known zeolite structures; for example, 4 (S4R), 6 (S6R), and 8 (S8R)-member single ring, 4-4 (D6R), 8-8 (D8R)-member double rings. The topologies of these units are shown in Figure 3.2 [Bekkum *et al.* (1991)]. Also listed are the symbols used to describe them. Most zeolite framework can be generated from several different SBU's. Descriptions of known zeolite structures based on their SBU's are listed in table 3.1 [Szoztak (1989)]. Both zeolite ZSM-5 and Ferrierite and described by their 5-1 building units. Offertile, zeolite L, Cancrinite, and Erionite are generated using only single 6-member rings. Some zeolite structttures can be described by several building units. The sodalite framework can be built from either the single 6-member ring or the single 4-member ring. Faujasite (type X or type Y) and zeolite A can be constructed using 4 ring or 6 ring building units. Zeolite A can also be formed using double 4 ring building units, whereas Faujasite cannot

Zeolite may be represented by the general formula,

$$M_{x/n}[(AlO_2)_x(SiO_2)_y]wH_2O$$
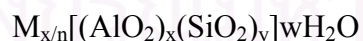
Where the term in brackets is the crystallographic unit cell. The metal cation of valence n is present to produce electrical neutrality since for wash aluminum tetrahedron in the lattice there is an overall charge of -1 [Tanake *et al.* (1989)]. M is a proton, the zeolites becomes a strong Bronsted acid. As catalysts, zeolite are unique in their ability to discriminate between reactant molecular size and shape [Barthoment (1984)].

Table 3.1 Zeolites and their secondary building units. The nomenclature used is consistent with that presented in Figure 3.2 [Szoztak (1989)]

ZEOLITE	SECONDARY BUILDING UNITS								
	4	6	8	4-4	6-6	8-8	4-1	5-1	4-4=1
Bikitaite								X	
Li-A (BW)	X	X	X						
Analcime	X	X							
Yagawaralite	X		X						
Episitbite								X	
ZSM-5								X	
ZSM-11								X	
Ferrierite								X	
Dachiardite								X	
Brewsterite	X								
Laumonite		X							
Mordenite								X	
Sodalite	X	X							
Henulandite									X
Stibite									X
Natrolite							X		
Thomsonite							X		
Edingtonite							X		
Cancrinite		X							
Zeolite L		X							
Mazzite	X								
Merlinoite	X		X			X			
Philipsite	X		X						
Zeolite Losod		X							
Erionite	X	X							
Paulingite	X								
Offretite		X							
TMA-E(AB)	X	X							
Gismondine	X		X						
Levyne		X							
ZK-5	X	X	X		X				
Chabazite	X	X			X				
Gmelinite	X	X	X		X				
Rho	X	X	X			X			
Type A	X	X	X	X					
Faujasite	X	X			X				
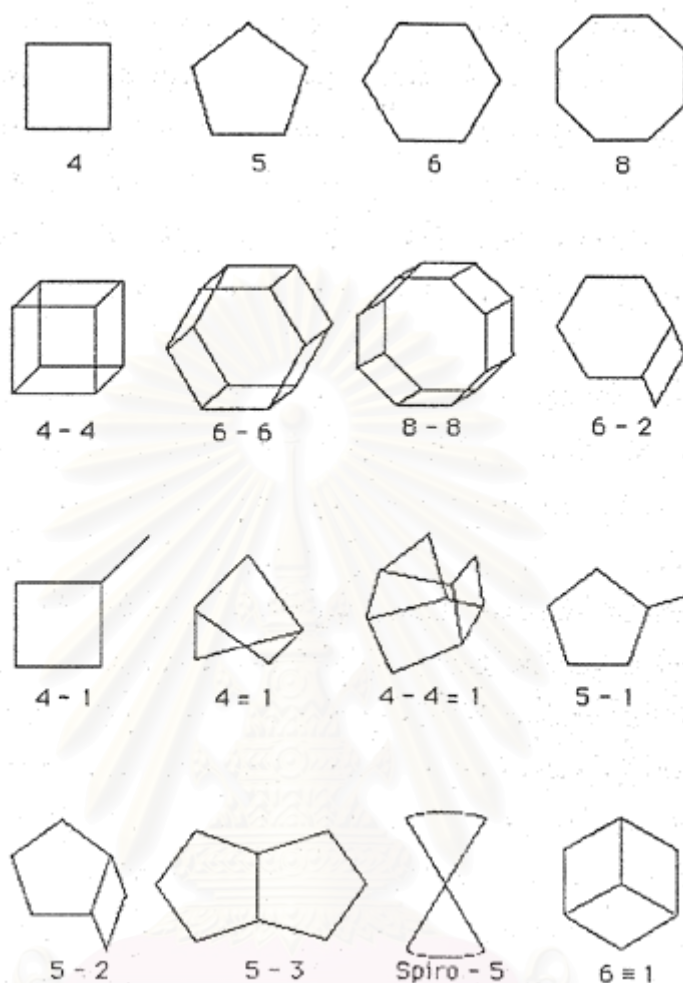
Figure 3.2 Secondary building units (SBU's) found in zeolite structures [Bekkum *et al.* (1991)]

3.3 Category of zeolite

There are over 40 known natural zeolites and more than 150 synthetic zeolites have been reported [Meier and Olson (1992)]. The number of synthetic zeolites with new structure morphologies grows rapidly with time. Based on the size of their pore opening, zeolites can be roughly divided into five major categories, namely 8-, 10- and 12-member oxygen ring systems, dual pore systems and mesoporous systems [Chen *et al.* (1996)]. Their pore structures can be characterized by crystallography, adsorption measurements and/or through

diagnostic reactions. One such diagnostic characterization test is the "constraint index" test. The concept of constraint index was defined as the ratio of the cracking rate constant of n-hexane to 3-methylpentane. The constraint index of a typical medium-pore zeolite usually ranges from 3 to 12 and those of the large-pore zeolites are in the range 1-3. For materials with an open porous structure, such as amorphorous silica alumina, their constraint indices are normally less than 1. On the contrary, small-pore zeolites normally have a large constraint index; for example, the index for erionite is 38.

A comprehensive bibliography of zeolite structures has been published by the International Zeolite Association [Meier and Olson (1992)]. The structural characteristics of assorted zeolites are summarized in table 3.2.

Zeolites with 10-membered oxygen rings normally possess a high siliceous framework structure. They are of special interest in industrial appications. In fact, they were the first family of zeolites that were synthesized with organic ammonium salts. With pore openings close to the dimensions of many organic molecules, they are particularly useful in shape selective catalysis. The 10-membered oxygen ring zeolites also possess other important characteristic properties including high activity, high tolerance to coking and high hydrothermal stability. Among the family of 10-membered oxygen ring zeolites, the MFI-type (ZSM-5) zeolite (Figure 3.3) is probably the most useful one.

Although the 10-membered oxygen ring zeolites were found to possess remarkable shape selectivity, catalysis of large molecules may require a zeolite catalyst with a large-pore opening. Typical 12-membered oxygen ring zeolites, such as faujasite-type zeolites, normally have pore opening greater than 5.5 A° and hence are more useful in catalytic applications with large molecules, for example in trimethylbenzene (TMB) conversions. Faujasite (X or Y ;Figure 3.4) zeolites can be synthesized using inorganic salts and have been widely used in catalytic cracking sincee the 1960s. The framework structures of zeolite beta and ZSM-12 are shown in Figure 3.5 and Figure 3.6, respectively.

Table 3.2 structural characteristics of selected zeolites [Tsai *et al.* (1991)].

Zeolite	Number of rings	Pore opening (Å)	Pore/channel structure	Void volume (ml/g)	D_{Frame}[a] (g/ml)	CI[b]
8-membered oxygen ring						
Erionite	8	3.6×5.1	Intersecting	0.35	1.51	38
10-membered oxygen ring						
ZSM-5	10	5.3×5.6 5.1×5.5	Intersecting	0.29	1.79	8.3
ZSM-11	10	5.3×5.4	Intersecting	0.29	1.79	8.7
ZSM-23	10	4.5×5.2	One-dimensional	-	-	9.1
Dual pore system						
Ferrierite (ZSM-35, FU-9)	10,8	4.2×5.4 3.5×4.8	One-dimensional 10:8 intersecting	0.28	1.76	4.5
MCM-22	12 10	7.1 Elliptical	Capped by 6 rings	-	-	1-3
Mordenite	12 8	6.5×7.0 2.6×5.7	One-dimensional 12:8 intersecting	0.28	1.70	0.5
Omega (ZSM-4)	12 8	7.4 3.4×5.6	One-dimensional One-dimensional	-	-	2.3 0.6
12-membered oxygen ring						
ZSM-12	12	5.5×5.9	One-dimensional	-	-	2.3
Beta	12	7.6×6.4 5.5×5.5	Intersecting	-	-	0.6
Faujasite (X,Y)	12 12	7.4 7.4×6.5	Intersecting 12:12 intersecting	0.48	1.27	0.4
Mesoporous system						
VPI-5	18	12.1	One-dimensional	-	-	-
MCM41-S	-	16-100	One-dimensional	-	-	-

[a]Framework density

[b]Constraint index

Zeolites with the dual pore system normally possess interconnecting pore channels with two different pore opening sizes. Mordenite is the well-known dual pore zeolite having a 12-membered oxygen ring channel with pore opening 6.5*7.0 A° which is interconnected to 8-membered oxygen ring channel with opening 2.6*5.7 A° (Figure 3.7). MCM-22, which was found more than 10

years, also possesses a dual pore system. Unlike Mordenite, MCM-22 consists of 10- and 12-membered oxygen rings (Figure 3.8) and thus shows prominent potential in future applications.
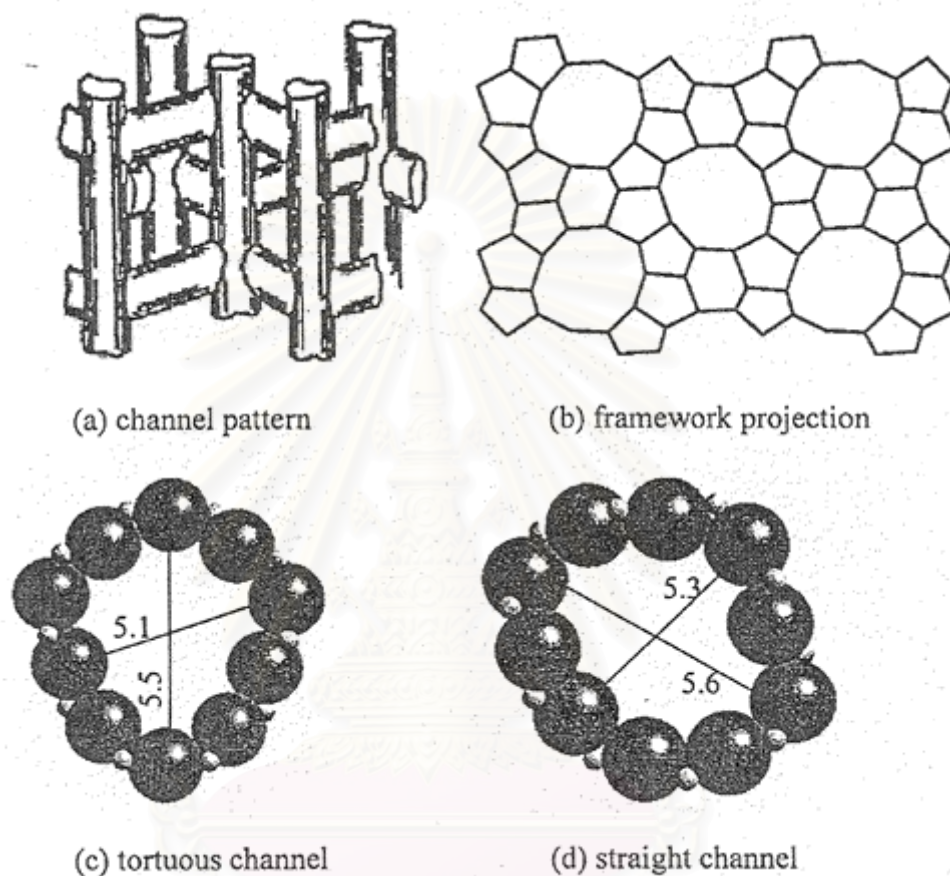

(a) channel pattern

(b) framework projection

(c) tortuous channel

(d) straight channel

Figure 3.3 Structure of ZSM-5 [Meier and Olson (1992)]

In the past decade, many research efforts in synthetic chemistry have been invested in the discovery of large-pore zeolite with pore diameter greater than 12-membered oxygen rings. The recent discovery of mesoporous materials with controllable pore opening (from 12 to more than 100 A°) such as VPI-5, MCM-41S undoubted will shed new light on future catalysis applications.

(a) framwork structure   (b) pore opening
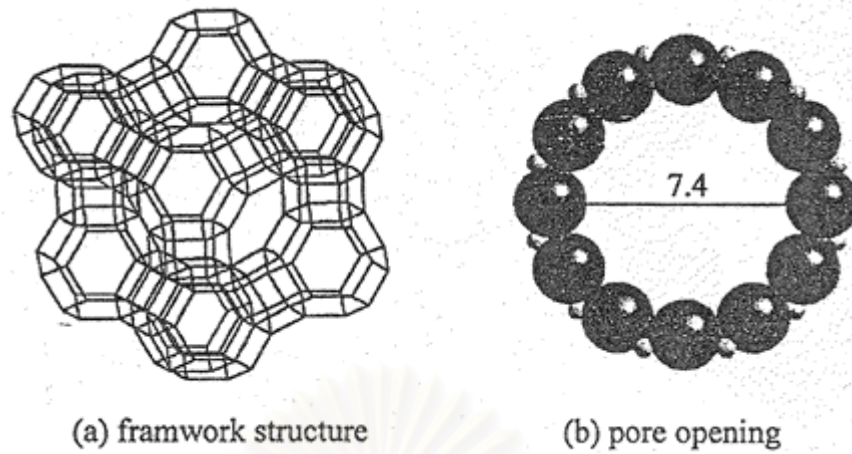
Figure 3.4 Structure of Faujasite [Meier and Olson (1992)]

(a) framework structure   (b) framework projection

(c) tortuous channel   (d) straight channel
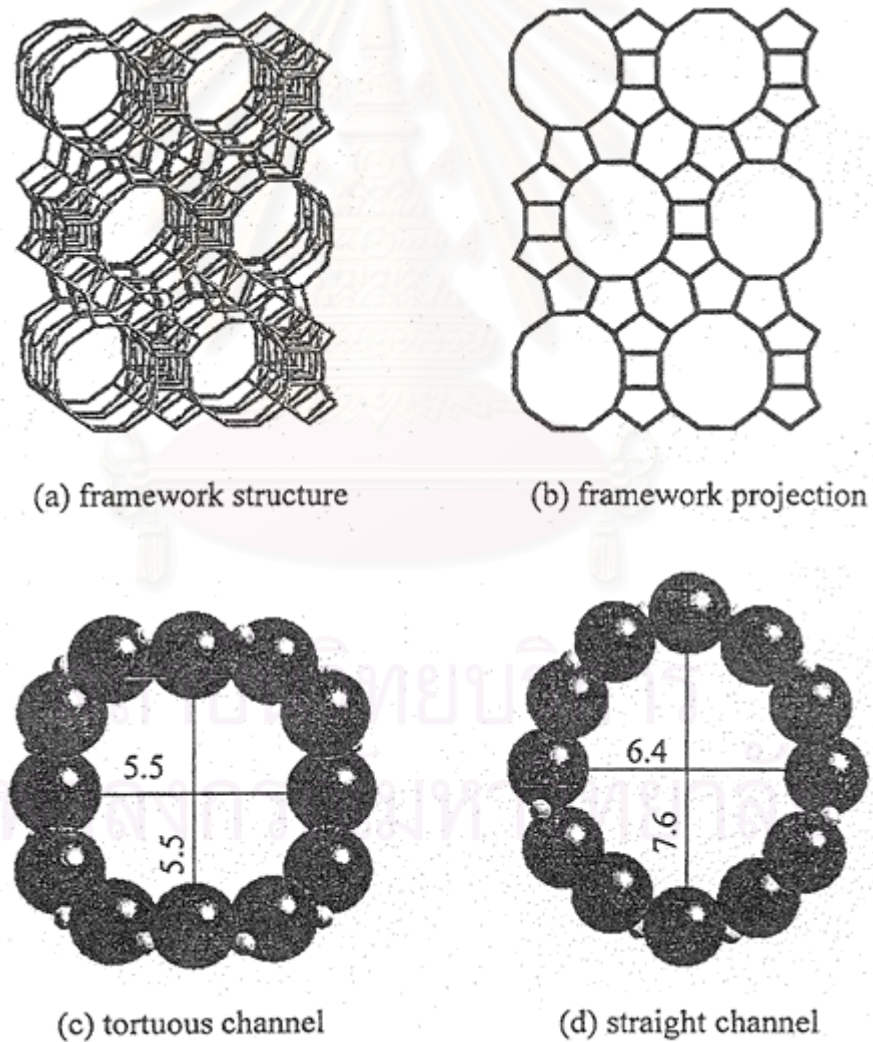
Figure 3.5 Structure of beta zeolite [Meier and Olson (1992)]

(a) framework projection   (b) pore opening
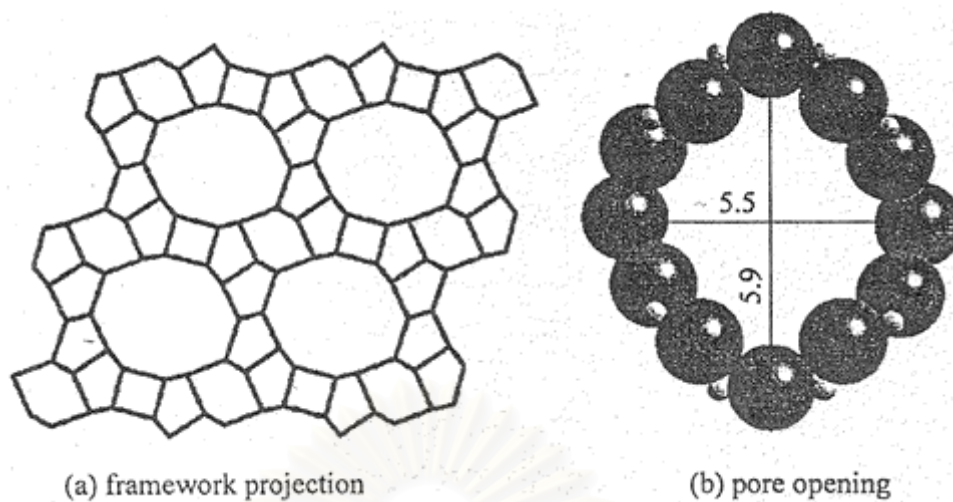
Figure 3.6 Structure of ZSM-12 [Meier and Olson (1992)]

(a) framework projection   (b) pore opening
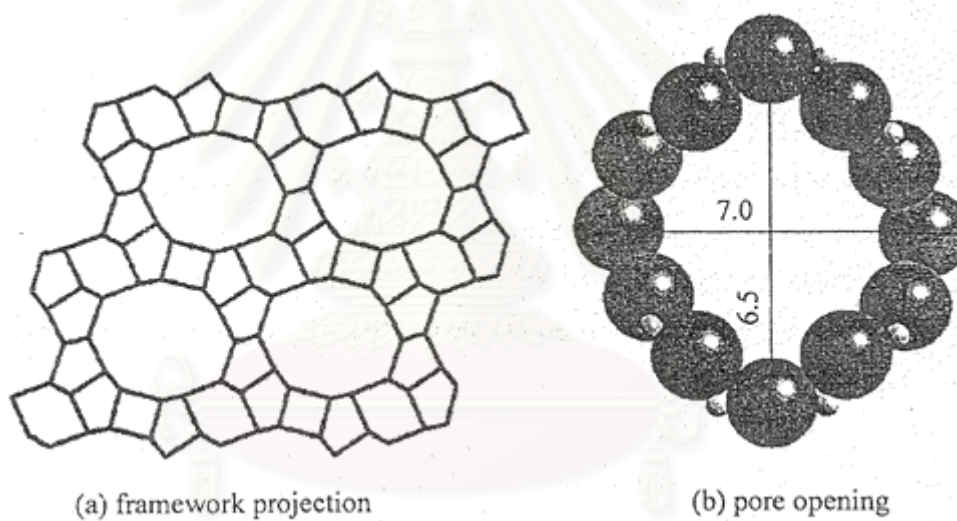
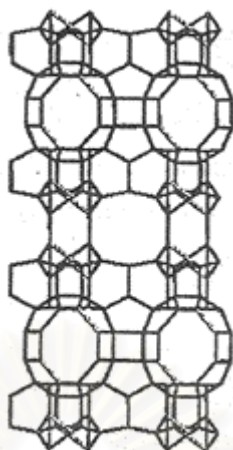**Figure 3.7** Structure of Mordenite [Meier and Olson (1992)]

Figure 3.8 Framework structure of MCM-22 [Meier and Olson (1992)]

3.4 Zeolite Active Sites

3.4.1 Acid sites

Classical Bronsted and Lewis acid models of acidity have been used to Classify. The active sites on zeolites. Bronsted acidity is proton donor acidity; a tridiagonally coordinated alumina atom is an electron deficient and can accept an electron pair, therefore behaves as a Lewis acid [Barthoment (1984), Ashton *et al.* (1985)].

In general, the increase in Si/Al ratio will increase acidic strength and thermal stability of zeolites [Sano *et al.* (1987)]. Since the numbers of acidic OH groups depend on the number of aluminum in zeolites framework, decrease in Al content is expected to reduce catalytic activity of zeolite. If the effect of increase in the acidic centers, increase in Al content, shall result in enhancement of catalytic activity.

Based on electrostatic consideration, the charge density at a cation site increases with increasing Si/Al ratio. It was conceived that these phenomena are related to reduction of electrostatic interaction between framework sites,

and possibly to difference in the order of aluminum in zeolite crystal – the location of Al in crystal structure [Ashton *et al.* (1985)].

An improvement in thermal or hydrothermal stability has been ascribed to the lower density of hydroxy groups, which is parallel to that of Al content [Barthoment (1984)]. A longer distance between hydroxyl groups decreases the probability of dehydroxylation that generates defects on structure of zeolites.

3.4.2 Generation of Acid Centers

Protonic acid centers of zeolite are generated in various ways. Figure 3.9 depics the thermal decomposition of ammonium-exchanged zeolites yielding the hydrogen form [Szoztak (1989)]

The Bronsted acidity due to water ionization on polyvalent cations, described below, is depicted in Figure 3.10 [Tanake *et al.* (1989)].

$$M^{n+} + xH_2O \longrightarrow M(OH)_x^{(n-x)} + xH^+ \qquad (3.1)$$

The exchange of monovalent ions by polyvalent cations could improve the catalytic property. Those highly charged cations create very centers by hydrolysis phenomena. Bronsted acid sites are also generated by the reduction of transition metal cations. The concentration of OH groups of zeolite containing transition metals was note to increase by hydrogen at 250-450 °C to increase with the rise of the reduction temperature [Tanake *et al.* (1989)].

$$Cu^{2+} + H_2 \longrightarrow Cu^0 + 2H^+ \qquad (3.2)$$
$$Ag^+ + 1/2H_2 \longrightarrow Ag^0 + H^+ \qquad (3.3)$$
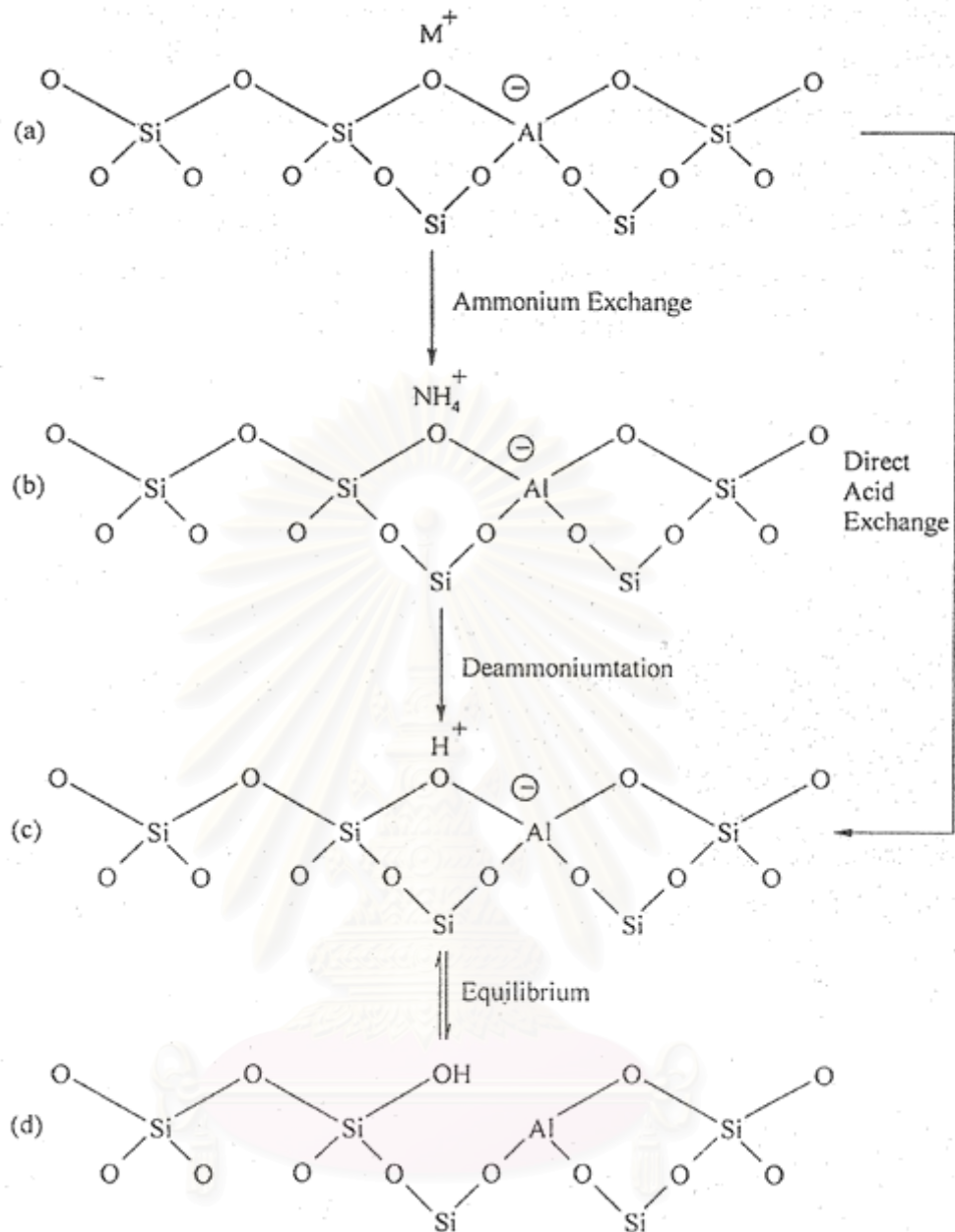
Figure 3.9 Diagram of the surface of a zeolite framework [Szoztak (1989)]

a) In the as-synthesis form M^+ is either an organic cation cation or an alkali metal cation.

b) Ammonium in exchange produces the NH_4^+ exchanged form.

c) Thermal treatment is used to remove ammonia, producing the H^+, acid form.

d) The acid form in c) is in equilibrium with the form shown in d), where there is a silanol group adjacent to tricoordinate aluminum.

The formation of Lewis acidity from Bronsted acid sites is depicted in Figure 3.11 [Tanake *et al.* (1989)]. The dehydretion reaction decreases the number of protons and increases that of Lewis sites. Bronsted (OH) and Lewis (-Al-) sites can be present simultaneously in the structure of zeolite at high temperature. Dehydroxylation is thought to occure in ZSM-5 zeolite above 500 °C and calcinations at 800 to 900 °C produces irreversible dehydroxylation, which causes defection in crystal structure of zeolite.
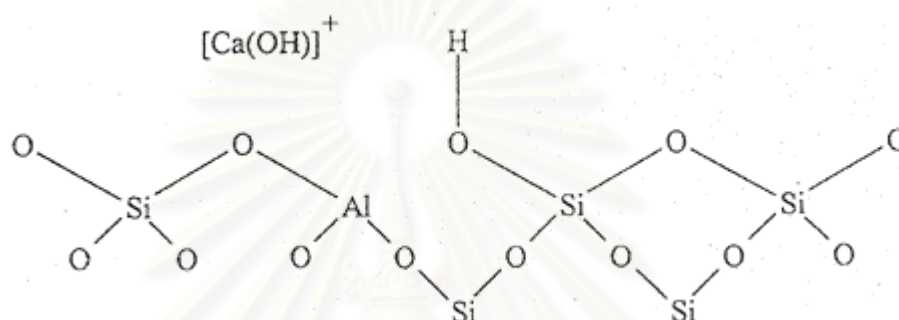

Figure 3.10 Water molecules co-ordinated to polyvalent cation are dissociated by heat treatment yielding Bronsted acidity [Tanake *et al.* (1989)].
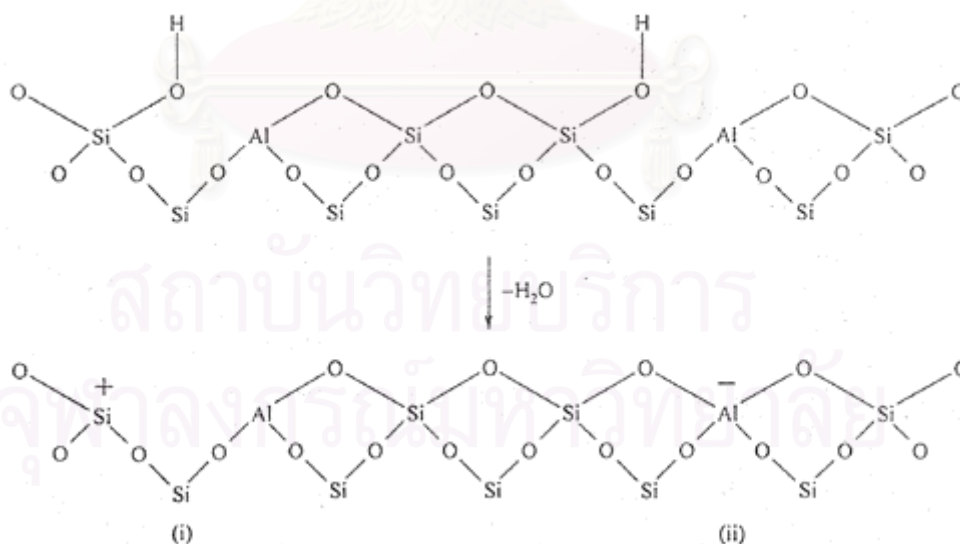

Figure 3.11 Lewis acid site developed by dehydroxylation of Bronsted acid site [Tanake *et al.* (1989)].

Dealumination is believed to occur during dehydroxylation which may result from the steam generation within the sample. The dealumination is indicated by an increase in the surface concentration of aluminum on the crystal. The dealumination process is expressed in Figure 3.12. The extent of dealumination monotonously increases with the partial pressure of steam.
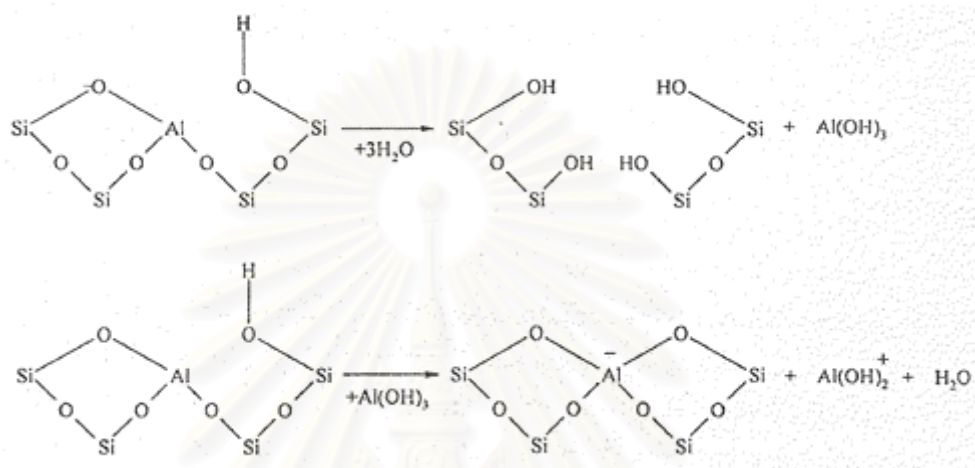
Figure 3.12 Steam dealumination process in zeolite [Tanake *et al.* (1989)].
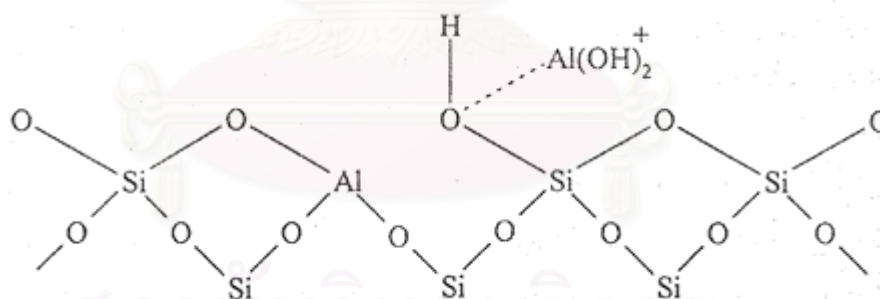
Figure 3.13 The enhancement of the acid strength of OH groups by their interaction with dislodged aluminum species [Tanake *et al.* (1989)].

The enhancement of the acid strength of OH groups is recently proposed to be pertinent to their interaction with those aluminum species sites tentatively expressed in Figure 3.13 [Tanake *et al.* (1989)]. Partial dealumination might therefore yield a catalyst of higher activity while severe steaming reduces the catalytic activity.

3.4.3   Basic Sites

In certain instances reactions have been shown to be catalyzed at basic (cation) site in zeolite without any influences from acid sites. The best-characterized example of this is that K-Y which splits n-hexane isomers at 500 °C. The potassium cation has been shown to control the unimolecular cracking (β- scission). Free radical mechanisms also contribute to surface catalytic reactions in these studies.

3.5 Shape Selective

Many reactions involving carbonium intermediates are catalyzed by acidic zeolites. With respect to a chemical standpoint the reaction mechanisms are not fundamentally different with zeolites or with any other acidic oxides. What zeolite add is shape selectivity effect. The shape selectivity characteristics of zeolites influence their catalytic phenomena by three modes; reactants shape selectivity, products shape selectivity and transition states shape selectivity. These types of selectivity are illustrated in Figure 3.14 [Szoztak (1989)].

Reactants of charge selectivity results from the limited diffusibility of some of the reactants, which cannot effectively enter and diffuse inside crystal pore structures of the zeolites. Product shape selectivity occurs as slowly diffusing product molecules cannot escape from the crystal and undergo secondary reactions. This reaction path is established by monitoring changes in product distribution as a function of varying contact time.

Restricted transition state shape selectivity is a kinetic effect arising from local environment around the active site, the rate constant for a certain reaction mechanism is reduced of the shape required for formation of necessary transition state is restricted.
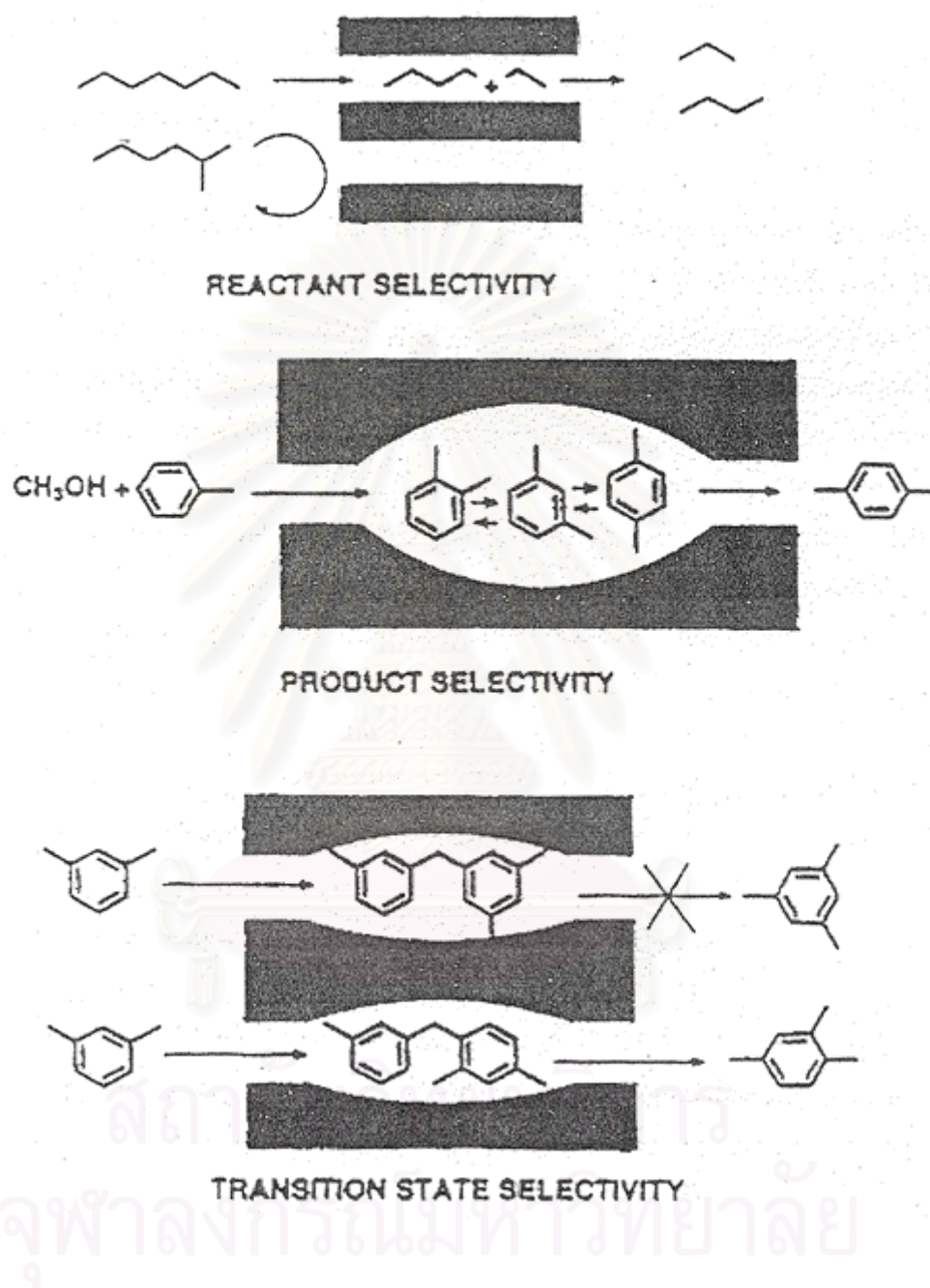
Figure 3.14 Diagram depicting the three type of selectivity [Szoztak (1989)]
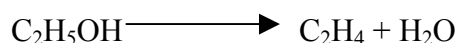
The critical diameter (as opposed to the length) of the molecules and the pore channel diameter of zeolites are important in predicting shape selective effects. However, molecules are deformable and can pass through openings, which are smaller than their critical diameters. Hence, not only size but also the dynamics and structure of the molecules must be taken into account.

3.6 ZSM-5 Zeolite

ZSM-5 zeolite has two   types of channel systems of similar size, one with a straight channel of pore opening 5.3*5.6 A° and the other with a tortuous channel of pore opening 5.1*5.5 A°. Those intersecting channels are perpendicular to each other, generating a three-dimensional ramework. ZSM-5 zeolites with a wide range of SiO_2/Al_2O_3 ratio can easily be synthesized. High siliceous ZSM-5 zeolites are more hydrophobic and hydrothermally stable compared to many other zeolites. Although the first synthetic ZSM-5 zeolite was discovered more than two decades ago (1972) new interesting applications are still emerging to this day. For example, its recent application in NO_x reduction, especially in the exhaust of lean-burn engine, has drawn much attention. Among various zeolite catalysts, ZSM-5 zeolite has the greatest number of industrial applications, covering from petrochemical production and refinery processing to environmental treatment.

3.7 The Dehydration of Ethanol

The dehydration of ethanol on Fe-ZSM-5 requires a high temperature. Ethylene is typically to be produced via a simultaneous parallel-consecutive scheme involving direct ethanol conversion [Tsao and Reilly (1978)].

$$C_2H_5OH \longrightarrow C_2H_4 + H_2O$$

As well as by the consecutive reaction

$$2C_2H_5OH \longrightarrow C_2H_5OC_2H_5 \longrightarrow 2\,C_2H_4 + 2H_2O$$

At low temperatures, diethyl ether is produced in significant quantities, while, at the high temperatures ethylene is the dominant product. [Berteau *et al.* (1987)].

Reaction network among ethanol, diethyl ether and ethylene on steam-treated and ZSM-5 catalysts using aqueous ethanol feeds may be represented by the following triangular scheme [Nguyen and Le Van Mao (1990)]:

$$-H_2O \ (1)$$
$$C_2H_5OH \longleftrightarrow C_2H_5OC_2H_5$$
$$-H_2O \ (3) \qquad\qquad -H_2O \ (2)$$
$$C_2H_4$$
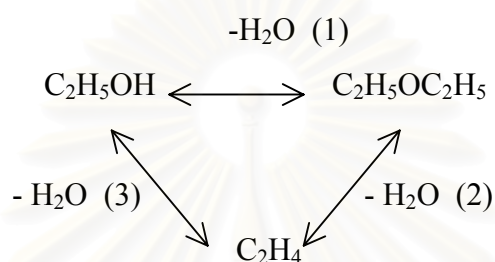
Operating under high temperature, producing ethylene (forward of reaction (3)) and diethyl ether (forward of reaction (1)). Although products such as diethyl ether, propene and other hydrocarbons were also detected, the reaction forming these byproducts were neglected and the effect of percentage of iron in ZSM-5 was investigated.

CHAPTER IV
EXPERIMENTAL

This chapter describes the experimental systems and the experimental procedures in this research. A describtion of catalyst preparation method is given in section 4.1. The metal loading by ion exchange, dehydration of ethanol and characterization of the catalysts are explained in section 4.2, 4.3 and 4.4, respectively. Details of experimental procedures, including the materials and apparatus are as follows.

The scope of this study

The catalysts used in dehydration of ethanol in this study were prepared by ion-exchange method and rapid crystallization method.

The catalyst are as follows:
- H-ZSM-5
- (1-7 Wt%) Fe-ZSM-5 by ion-exchange method
- 5 Wt% Fe-ZSM-5 by rapid crystallization method

Ethanol conversion was carrier out under the following conditions:

reaction temperature	: 400-600 °C
operation pressure	: 1 atm
time of ethanol conversion	: 0-60 min.
GHSV of ethanol	: 2000-6000 h^{-1}

4.1 Catalyst preparation

ZSM-5, Fe-ZSM-5 catalyst having various percentage of iron were prepared. The $AlCl_3$ was replaced by $Fe(NO_3)_3.9H_2O$ at the stage of gel formation and TPABr (Tetra-n-Propyl Ammonium Bromide) $[((CH_3CH_2CH_2)_4N)Br]$ was used as an organic template in the rapid crystallization method for H-ZSM-5 synthesis [Inui and T. Yamase (1984)]. The preparation procedures and

the reagents used are shown in Figure 4.1 and Table 4.1, respectively. (For calculation see Appendix A-1)

4.1.1 *Preparation of Gel Precipitation and Decantation Solution*

The source of metal was $AlCl_3$. TPABr (Tetra-n-Propyl Ammonium Bromide) $[((CH_3CH_2CH_2)_4N)Br]$ was used as an organic template. The atomic ratio of silicon/Aluminium was set at 40. The preparation of the supernatant liquid was separated from that of gel, which was important to prepare the uniform crystals. The detail procedures were as follows : Firstly, a gel mixture was prepared by adding G1-solution and G2-solution into G3-solution while stirring with a magnetic stirrer (Figure 4.2) at room temperature. G1-solution and G2-solution was added from burette by the manual control to keep the pH of the mixed solution in the range of 9-11, since it is expected that this pH value is suitable for precipitation. The gel mixture was seperated from the supernatant liquid by using centrifuge.

The precipitated gel mixture was milled for totally 1 hr. by powder miller as shown in Figure 4.3. The milling procedure was follows : milled 20 min. and centrifuge (to remove the liquid out) about three times.

Milling the gel mixture before the hydrothermal treatment was essential to obtain the uniform and fine crystals. The gel precipitate was kept for mixing with the supernatant solution. On the other hand, another decantation solution was prepared by adding S1-solution and S2-solution into S3-solution. The method and condition of mixing were similar to the preparation of gel mixture. Upon the complete mixing the precipitating gel was then removed from the supernatant solution by the centrifuge and the supernatant solution was mixed altogether with the milled gel mixture, expecting that before mixing adjust the pH of solution between 9-11 with H_2SO_4 (conc.) or 1 M NaOH solution

Table 4.1 Reagents used for the catalysts preparation

Reagents for the gel preparation		Reagents for decant solution preparation	
Solution G1		**Solution S1**	
$AlCl_3$ (g)	2.2496	$AlCl_3$ (g)	2.2496
$Fe(NO_3)_3.9H_2O$	X	$Fe(NO_3)_3.9H_2O$	X
TPABr (g)	5.72	TPABr (g)	5.72
NaCl (g)	11.95	-	-
Distilled water (ml)	60	Distilled water (ml)	60
H_2SO_4 (conc.) (g)	3.40	H_2SO_4 (conc.) (g)	3.40
Solution G2		**Solution S2**	
Distilled water (ml)	45	Distilled water (ml)	45
Water glass (g)	69	Water glass (g)	69
Solution G3		**Solution S3**	
TPABr (g)	2.61	-	-
NaCl (g)	40.59	NaCl (g)	26.27
NaOH (g)	2.39	-	-
Distilled water (ml)	208	Distilled water (ml)	104
H_2SO_4 (conc.) (g)	1.55	-	-

4.1.2 Crystallization

The mixture of milling precipitate and the supernatant of decant solution was charged in litre stainless steel autoclave. The atmosphere in the autpoclave was replaced by nitrogen gas and pressurized up to 3 kg/cm^2 gauge. Then the mixture in the autoclave was heated from room temperature to 160 °C in 90 min. and then up to 210 °C in 4.2 hr while being stirred at 60 rpm, followed by cooling down the hot mixture to room temperature in the autoclave overnight. The temperature was programmed under the hydrothermal treatment to minimize the time which was necessary for the crystallization. The produced crystals were washed with distilled water, to remove Cl^- out of the crystals, about 8 times by using the centrifugal separator (about 10 min. for each time) and dried in an oven at 110 °C for at least 3 hr.
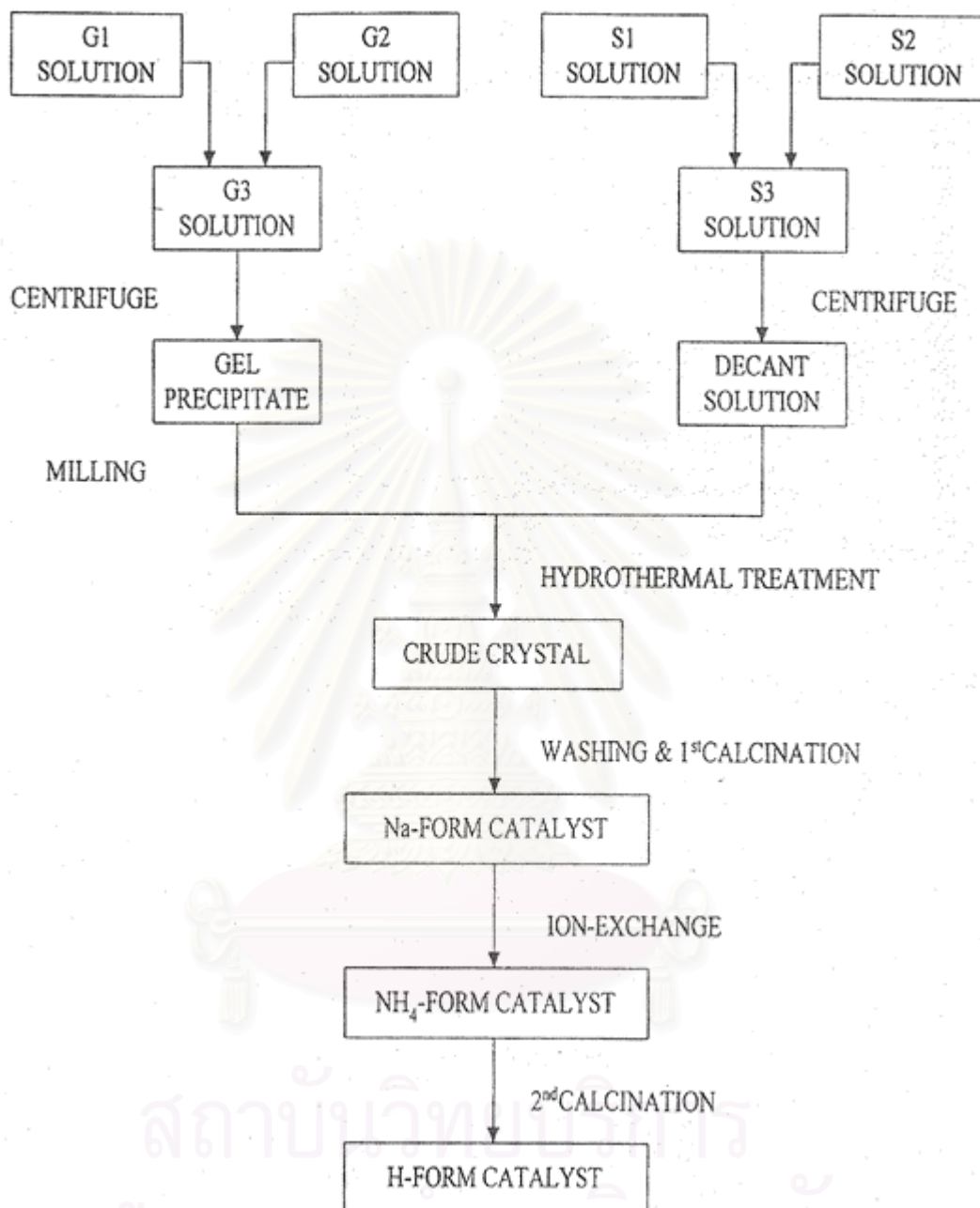
Figure 4.1 Preparation procedure of MFI catalysts by rapid crystallization
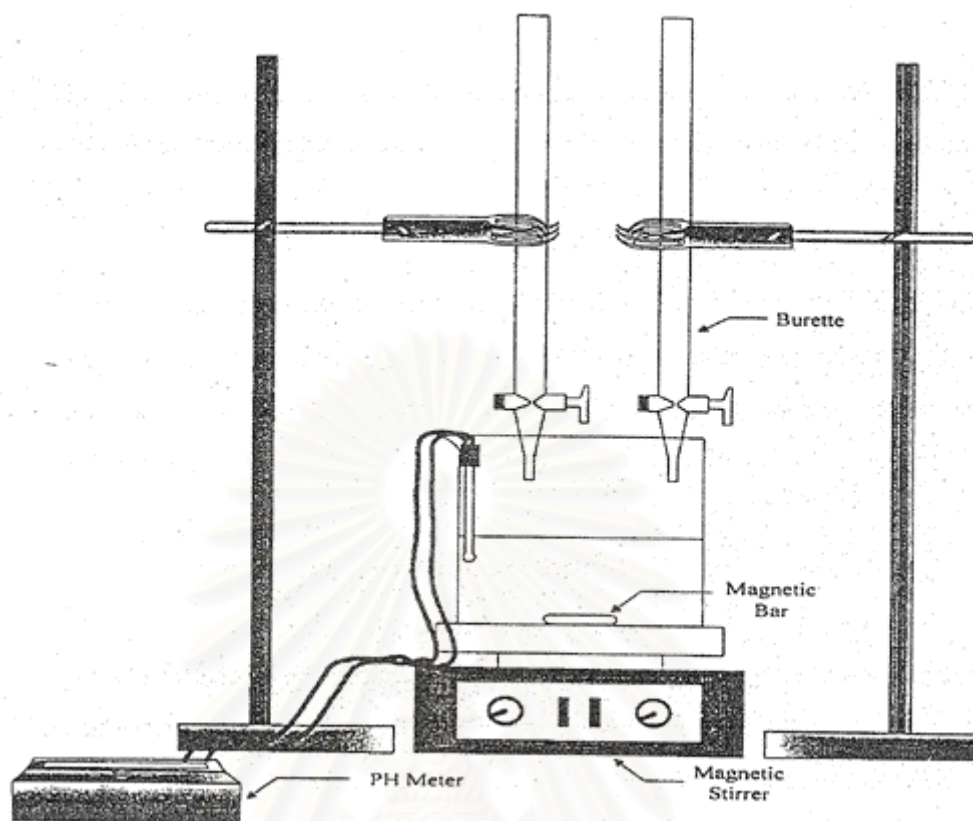
Figure 4.2 A set of apparatus used for preparation of supernatant solution and gel precipitation as providing for the rapid crystallization
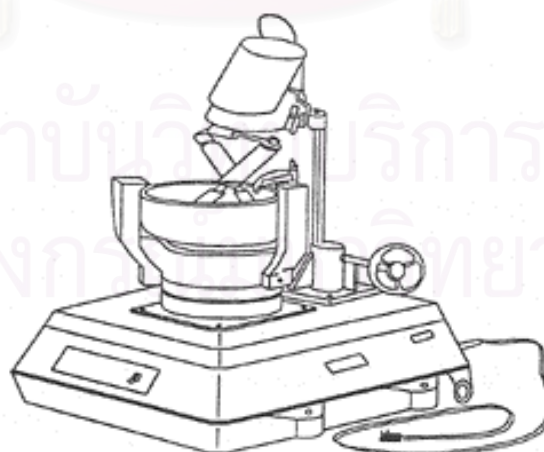

Figure 4.3 A powder miller (Yamato-Nitto, UT-22)

4.1.3   First Calcination

The dry catalysts in a porcelain was heated in a furnace under an air ambient from room temperature to 540 °C in 60 min. and then kept at this temperature for 3.5 hr.

At this step, the organic template (TPABr) was burned out and left the cavities and channels in the crystals. The calcined crystal was cooled to room temperature in a desiccator. After this step the crystals formed were called "Na-form catalyst".

4.1.4   Ammonium Ion-Exchange of Na-form Crystal

The ion-exchange step was carried out by mixing 3 g of Na-form catalyst with 90 ml of 1 M NH_4NO_3 and heated on a stirring hot plate at 80 °C for 40 min. After that, the mixture was cooled down to room temperature and washed with distilled water about 3 times by using the centrifugal separator (about 10 min. for each time). The ion-exchange step was repeated about 3 times. Then the ion-exchange crystal was dried at 110 °C for at least 3 hr. in an oven. The Na-form crystal was thus changed to "NH_4-form catalyst".

4.1.5   Second Calcination

The NH_4-form crystal was calcined in a furnace by heating from room temperature to 540 °C in 60 min. and then kept at this temperature for 3.5 hr. After this step the crystal thus obtained was called "H-form catalyst".

4.2 Metal Loading by Ion-Exchange

About 2 g of catalyst was immersed in 60 ml of metal salt aqueous solution at 100 °C for 3 hr. It was washed with distilled water about 5 times, about 10 min for each time (as shown in Figure 4.4). The sample was dried overnight at 110 °C. Finally, dry crystal was heated in air with the constant heating rate of 10 °C/min up to 350 °C and maintained for 2 hr.
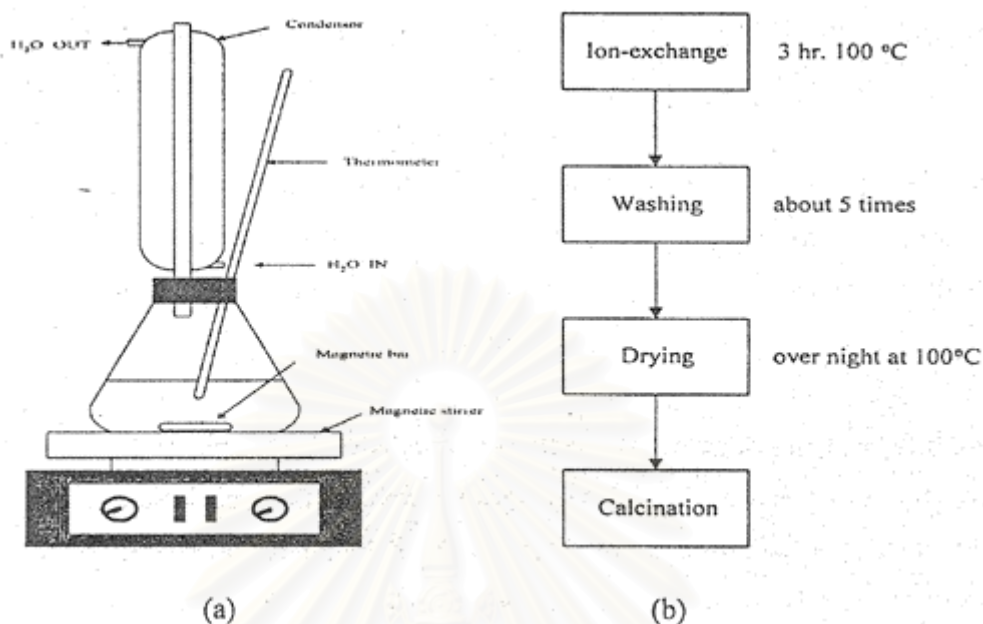
Figure 4.4 (a) A set of apparatus used for preparation of metal ion-exchanged
on catalyst

(b) A diagram for metal ion-exchanged on catalyst

The catalysts were tableted by a tablet machine. After that, the
catalysts were crushed and sieve to range of 8-16 mesh to provide the same
diffusion rate and the reaction.

4.3 Dehydration of Ethanol

4.3.1 Chemicals and Reagents

Ethanol available from Carlo Erba Reagenti

N_2(UHP) was supplied by Thai Industrial Gases Limited

4.3.2 Instruments and Apparatus

A flow diagram of the steady state ethanol conversion system is shown in Figure 4.5. The system consists of a reactor, an automation temperature controller, an electrical furnace and a gas control system. This instruments used in this system is listed and explained below :

1. Reactor : The reactor is a conventional microreactor made from a quartz tube with 6 mm inside diameter, so it can be operated at high temperature. The reaction was carried out under ordinary gas flow and atmospheric pressure.

2. Automation Temperature Controller : Thi consists of magnetic switch connected to a variable voltage transformer and a RKC temperature controller connected to a thermocouple attached to a catalyst bed in a reactor. A dial setting establishes a set point at any temperature with in the range between 0 to 800 °C

3. Electrical Furnace : This supplies the required heat to the reactor for reaction. The reactor can be operated from room temperature up to 700 °C at maximum voltage of 220 volts.

4. Gas Controlling System : nitrogen is equipped with a pressure regulator (0-120 psig). An on-off valve and a needle valve were used to adjust flow rate of gas.

5. Gas Chromatographs : The apparatus consist of flame ionization detectoe equipped with gas chromatographs, Shimadzu GC-14A and , Shimadzu GC-14B, and thermal conductivity detector equipped with gas chromatographs, , Shimadzu GC-8A. Operating condition used in this study are given in Table 4.2.

4.3.3   Reaction Method

The dehydration of ethanol reaction was carried out by using a conventional flow apparatus shown in Figure 4.5.

A 0.2 g of the catalyst was packed in the middle of a quartz tubular reactor. The reactor was then firmly placed into the furnace.

Table 4.2 Operating conditions for gas chromatograph.

Gas Chromatograph Detector	Shimadzu GC-14A FID	Shimadzu GC-14B FID	Shimadzu GC-8A TCD
Column	Capillary	VZ-10	MS-5A, Porapak-Q
Carrier gas	N_2 (99.999%)	N_2 (99.999%)	H_2 (99.999%)
Carrier gas flow	25 ml/min	25 ml/min	25 ml/min
Column temperature			
- initial	40	70	170
- final	140	70	170
Detector temperature	150	150	180
Injector temperature	150	100	180
Analyzed gas	Hydrocarbon	Hydrocarbon C_1-C_4	Ethanol

Dehydration of ethanol was carried out under the following condition : atmospheric pressure; gas hourly space velocity (GHSV), 2000-6000 hr^{-1}, reaction temperature, 400-600 °C

The procedure used to operate this reactor is as follows:

1. Adjust the outlet pressure of nitrogen to 1 kg/cm^2 and allow the gas to flow through a rotameter (see Appendix A-3), measure the outlet gas flow rate by using a bubble flowmeter.

2. Heat up the reactor (under N$_2$ Flow) by raising the temperature from room temperature to required temperature and then hold at that temperature for 60 min.

3. Put 20 Wt% ethanol 10 ml in a saturature

4. Start to run the reaction by adjusting 2 three-way valves to allow nitrogen gas to pass through ethanol inside the saturature set in the water bath, and at that time the reaction time is taken as zero.

5. Take sample to analyze at 1 hr. on stream. The reaction products were analyzed by FID-type gas chromatographs.
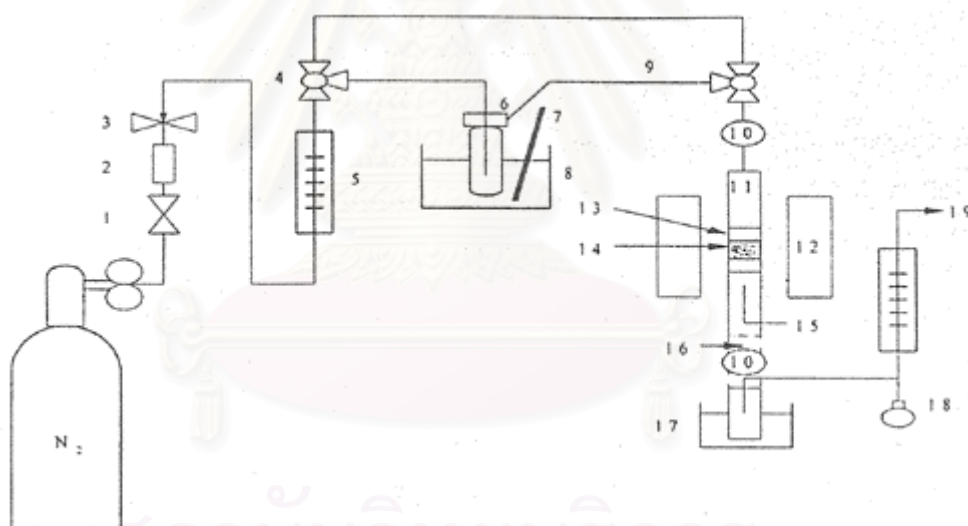
1.On-off valve	2.Gas filter	3.Needle valve	4.Three-way valve
5.Flow meter	6.Saturator	7.Thermocouple	8.Water bath
9.Heating line	10.Sampling port	11.Tubular reactor	12.Electric furnace
13.Quartz wool	14.Catalyst	15.Thermocouple	16.Heating tape
17.Trap	18.Soap-film flowmeter		19.Purge

Figure 4.5 Schematic diagram of the reaction apparatus for the dehydration of ethanol

4.4 Characterization of the catalysts

4.4.1 X-ray Diffraction Patterns

X-ray diffraction (XRD) patterns of the catalysts were performed with SIEMENS XRD D5000, accurately measured in the 5-40° 2θ angular region, at Petrochemical Engineering Research Laboratory, Chulalongkorn University.

4.4.2 Morphology

The shape and the distribution of size of the crystals were observed by JEOL Scanning Electron Microscope (SEM) at the Scientific and Technological Research Equipment Center, Chulalongkorn University (STREC).

4.4.3 BET Surface Area Measurement

Surface areas of the catalysts were measured by the BET method, with nitrogen as the adsorbate using a micrometritics model ASAP 2000 at liquid-nitrogen boiling point temperature at the Analysis Center of Department of Chemical Engineering, Faculty of Engineering, Chulalongkorn University.

4.4.4 Chemical Analysis

Percentage of metals was analyzed by X-ray fluorescence spectrometer (XRF) technique. The silicon, aluminum and iron contents of the prepared catalyst was analyzed by X-ray fluorescence spectrometer (XRF) at the Department of Science Service, Ministry of Science, Technology and Environment.

4.4.5 Acidity Measurement

Temperature programmed desorption of ammonia (NH_3-TPD) have been used to investigate the acidic properties of ZSM-5 zeolites. The acidity of

catalysts was analyzed by NH$_3$-TPD at the Institute of Research and Technology, PTT

CHAPTER V
RESULTS AND DISCUSSION

In this chapter, the results and discussion are classified into the major parts. Firstly, characterization of the H-ZSM-5 and Fe-ZSM-5 catalysts by XRD, SEM, BET, XRF and NH_3-TPD are described in section 5.1. Secondly, catalytic behavior of catalyst on the dehydration of ethanol is explained in section 5.2.

5.1 Catalyst Characterization

5.1.1 X-ray Diffraction Pattern

The X-ray diffraction patterns for the prepared catalysts are shown in Figure 5.1. All the XRD patterns of catalyst correspond well with those report in the literature. While other non-zeolite phases such as oxide phases of Fe was not detected. This indicates that all the catalysts have the same pentasil pore-opening structure as ZSM-5 and a little amount of metal loaded did not change the main structure of ZSM-5 catalyst.
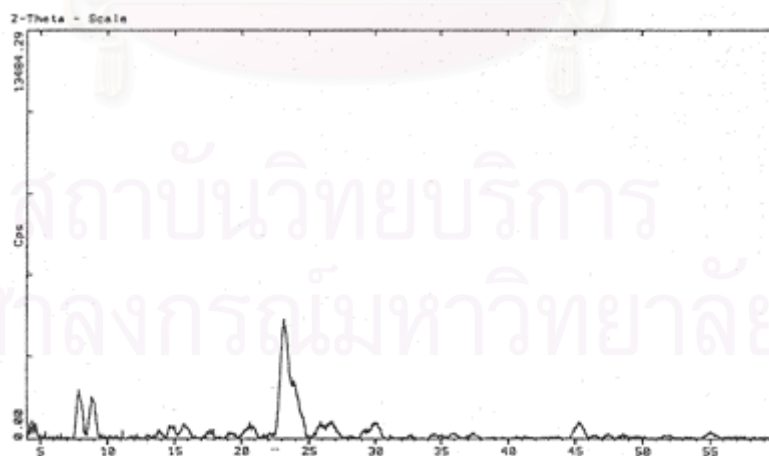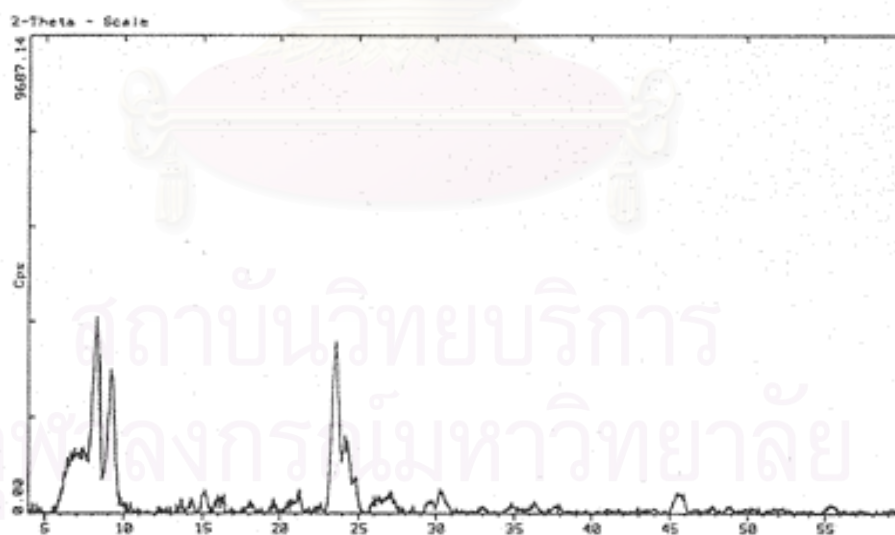

(a) Referent H-ZSM-5

Figure 5.1 The X-ray Diffraction of the Prepared Catalysts
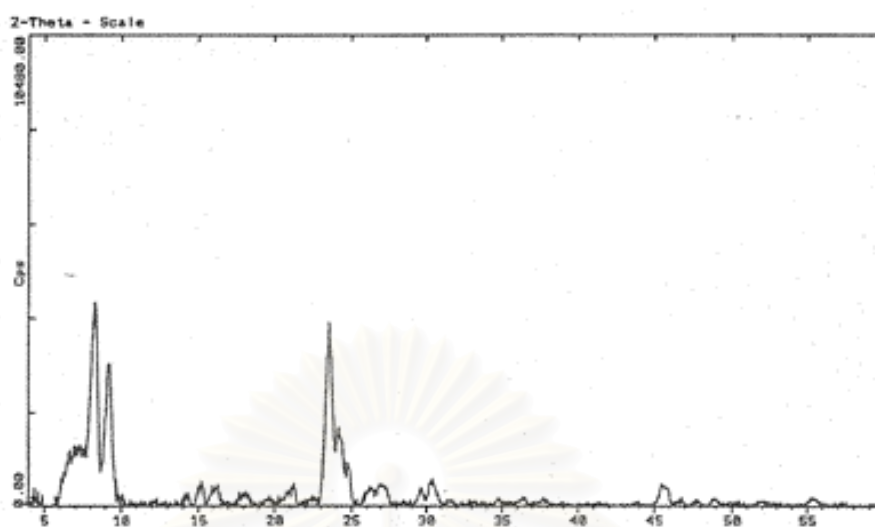
(b) H-ZSM-5

Figure 5.1 The X-ray Diffraction of the Prepared Catalysts

(c) 1%Fe-ZSM-5

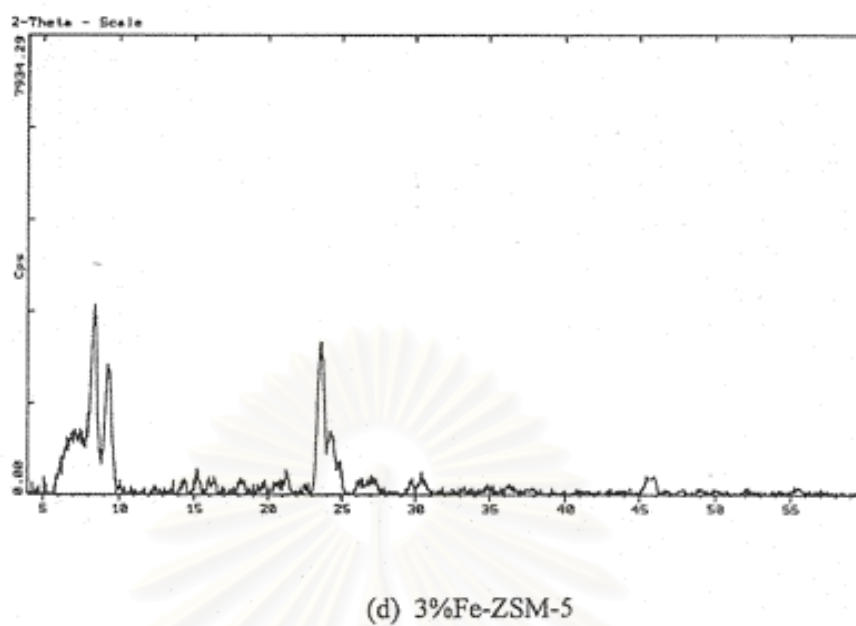**Figure 5.1** The X-ray Diffraction of the Prepared Catalysts

(d) 3%Fe-ZSM-5

Figure 5.1 The X-ray Diffraction of the Prepared Catalysts

(e) 5%Fe-ZSM-5
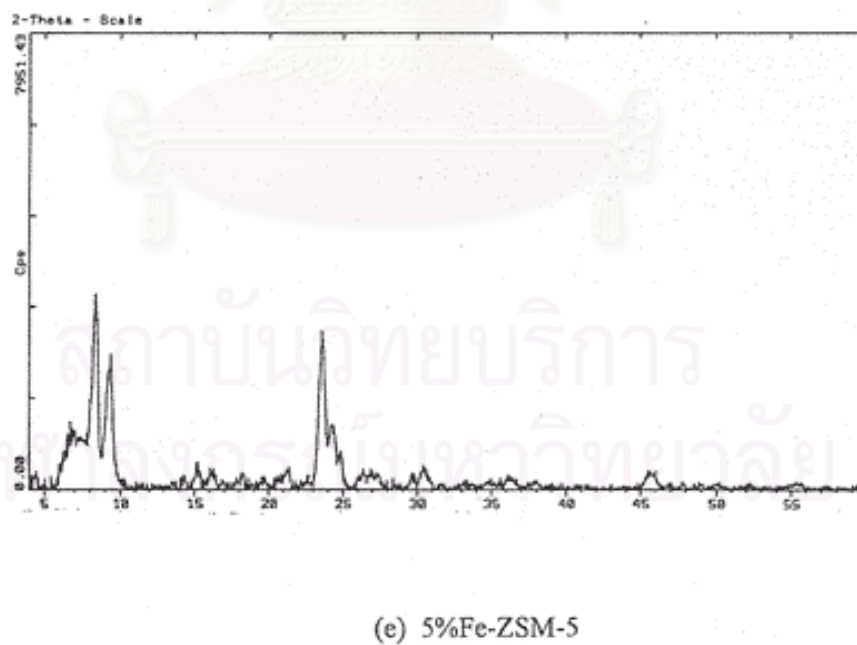
Figure 5.1 The X-ray Diffraction of the Prepared Catalysts
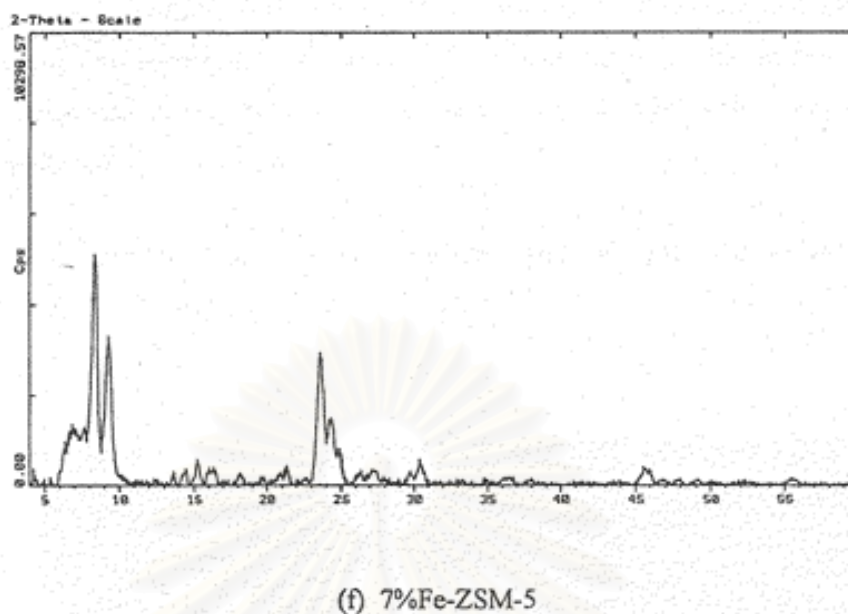
(f) 7%Fe-ZSM-5

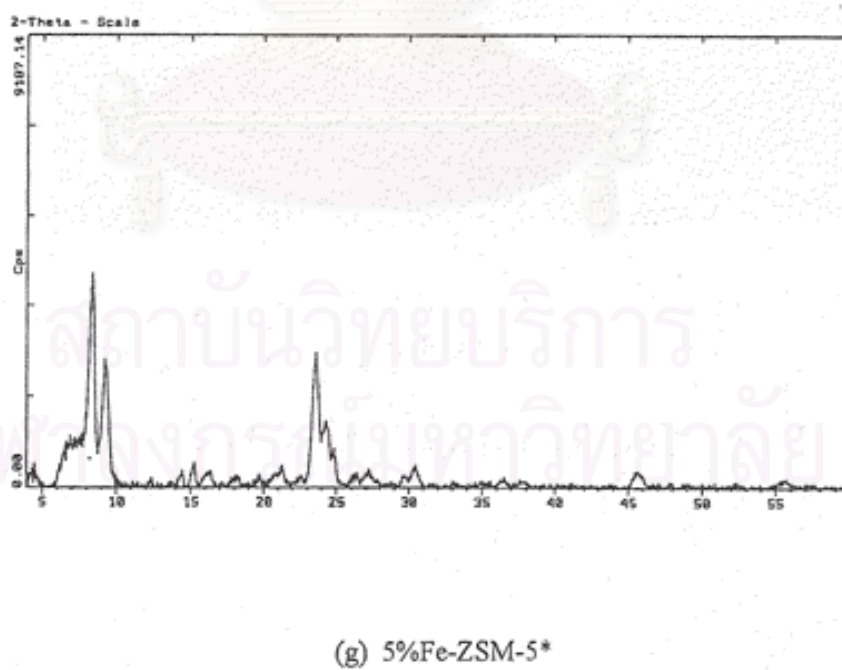**Figure 5.1** The X-ray Diffraction of the Prepared Catalysts

(g) 5%Fe-ZSM-5*

Figure 5.1 The X-ray Diffraction of the Prepared Catalysts

5.1.2   Morphology

Scanning Electron Microscope (SEM) photographs of the prepared catalysted are shown in Figure 5.2. As shown, the morphology of the whole samples were composed of tiny rectangular unit crystallites agglomerated to substantially hexagonal particle in shape.

The crystal sizes of ZSM-5 modified with Fe and unmodified ZSM-5 were approximately varied during 4-5 μm.
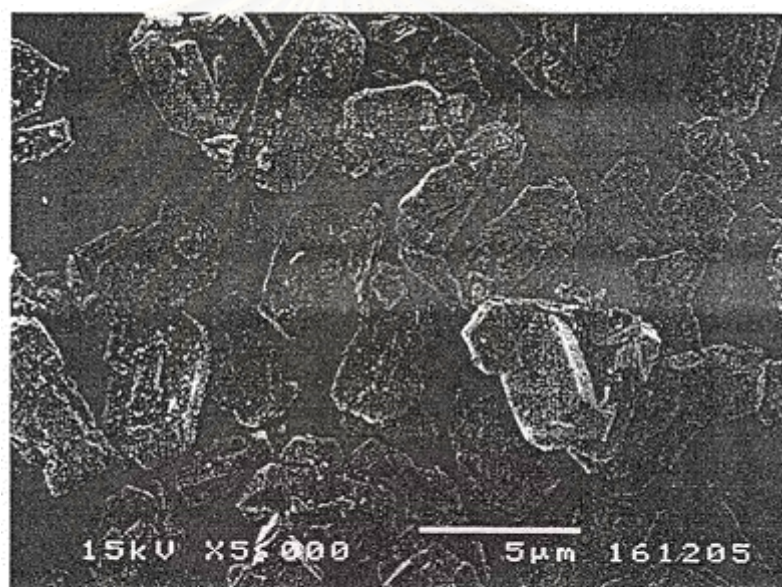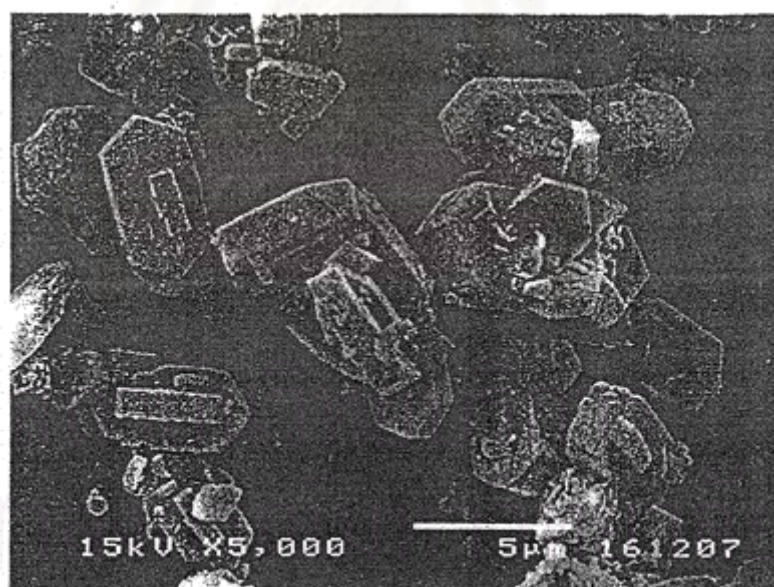

(a) H-ZSM-5

Figure 5.2 Scanning Electron Microscope (SEM) photographs

(b) 1%-ZSM-5

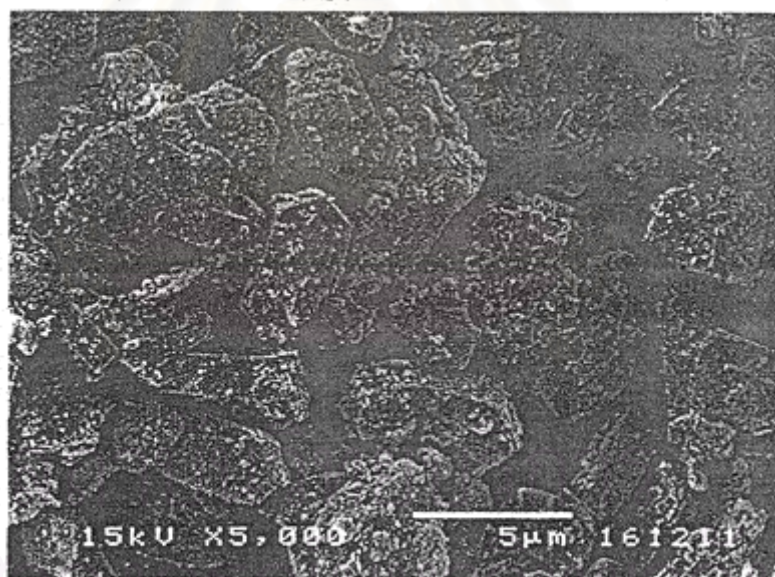**Figure 5.2** Scanning Electron Microscope (SEM) photographs

(c) 3%-ZSM-5

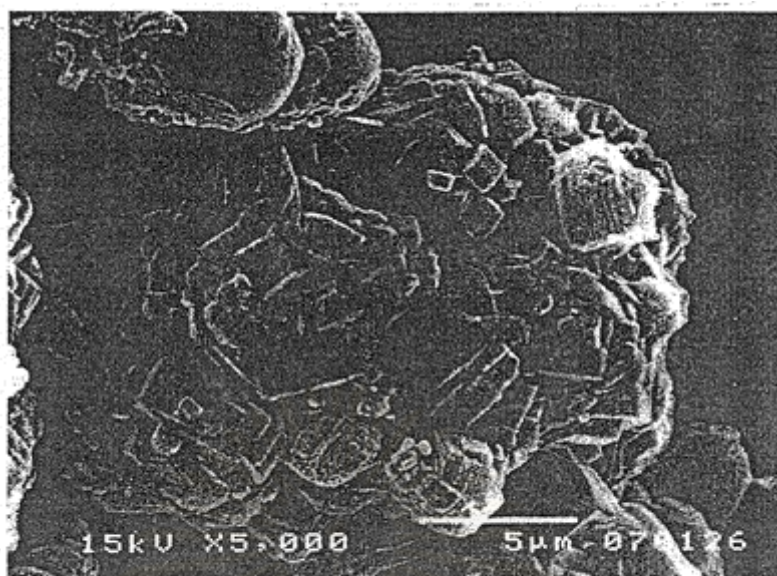**Figure 5.2** Scanning Electron Microscope (SEM) photographs

(d) 5%-ZSM-5

Figure 5.2 Scanning Electron Microscope (SEM) photographs

(e) 7%-ZSM-5

Figure 5.2 Scanning Electron Microscope (SEM) photographs

(f) 5%Fe-ZSM-5*

Figure 5.2 Scanning Electron Microscope (SEM) photographs

5.1.3   BET surface area

BET surface areas of the various prepared catalysts are shown in
Table 5.1.

Table 5.1 BET surface areas of the various prepared catalysts

Catalyst	BET surface areas (m^2/g of catalysts)
H-ZSM-5	230.3964
1%Fe-ZSM-5	219.1870
3%Fe-ZSM-5	220.6969
5%Fe-ZSM-5	229.7768
7%Fe-ZSM-5	216.8798
5%Fe-ZSM-5*	201.3425

*prepared by rapid crystallization

From Table 5.1, the BET surface areas after iron loading by ion-exchange method for 1-7%Fe-ZSM-5 and rapid crystallization method for 5%Fe-ZSM-5 was slightly decreased when Fe was load in.

This introduces the channel occupation of a small amount of metal or pore mouth blockage.

5.1.4 Chemical Composition

The results of the quantitative analysis of silicon, aluminum and iron in the synthesized crystals are shown in Table 5.2 and Table 5.3, respectively.

Table 5.2 Si/Al ratio in ZSM-5 zeolites

Catalyst	Si/Al ratio loaded	Si/Al ratio observed
H-ZSM-5	20	21.64
1%Fe-ZSM-5	20	17.28
3%Fe-ZSM-5	20	26.12
5%Fe-ZSM-5	20	20.37
7%Fe-ZSM-5	20	30.48
5%Fe-ZSM-5*	20	23.05

*prepared by rapid crystallization

Table 5.3 Fe contents in ZSM-5 zeolites

Catalyst	%Fe loaded	%Fe observed
H-ZSM-5	-	-
1%Fe-ZSM-5	1	1.32
3%Fe-ZSM-5	3	3.83
5%Fe-ZSM-5	5	5.18
7%Fe-ZSM-5	7	6.76
5%Fe-ZSM-5*	5	4.17

*prepared by rapid crystallization

5.1.4   Temperature Programmed Desorption of Ammonia (NH$_3$-TPD)

The TPD profile of desorbed NH$_3$ from iron loaded and non-loaded catalysts are shown in Table 5.4. The profile is composed of two peaks,i.e., a high temperature peak of strong acid sites and a low temperature peak of weak acid sites. [Inui, T.(1984)].

Table 5.4 The peak concentration of acid sites of the various prepared catalysts.

Catalysts	Peak concentration of strong acid sites	Peak concentration of weak acid sites
H-ZSM-5	0.48	0.19
1%Fe-ZSM-5	0.44	0.13
3%Fe-ZSM-5	0.37	0.07
5%Fe-ZSM-5	0.35	0.10
7%Fe-ZSM-5	0.34	0.11
5%Fe-ZSM-5*	0.32	0.09

*prepared by rapid crystallization

From Figure 5.3, the separation of high temperature and low temperature peaks was made at about 300 °C. For strong acid sites, the amount of the acidic site of metal loading on H-ZSM-5 were lower than the unmodified ZSM-5 catalyst. This indicates that the acid sites from the unmodified ZSM-5 were decreased by the iron loading on ZSM-5 catalyst.
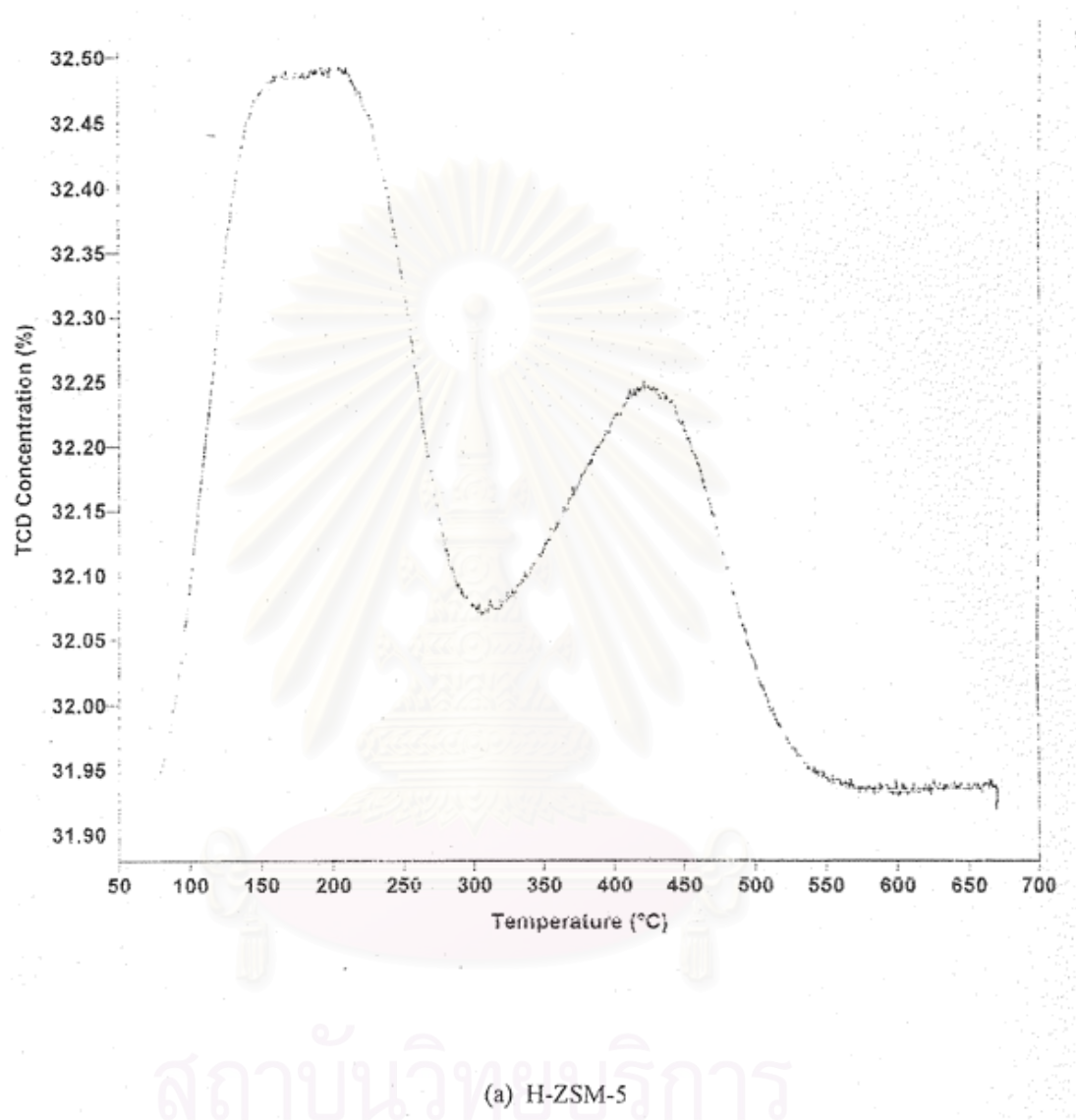
(a) H-ZSM-5

Figure 5.3 The Temperature Programmed Desorption Profile

(b) 1%Fe-ZSM-5

Figure 5.3 The Temperature Programmed Desorption Profile

(c) 3%Fe-ZSM-5

Figure 5.3 The Temperature Programmed Desorption Profile

(d) 5%Fe-ZSM-5

Figure 5.3 The Temperature Programmed Desorption Profile
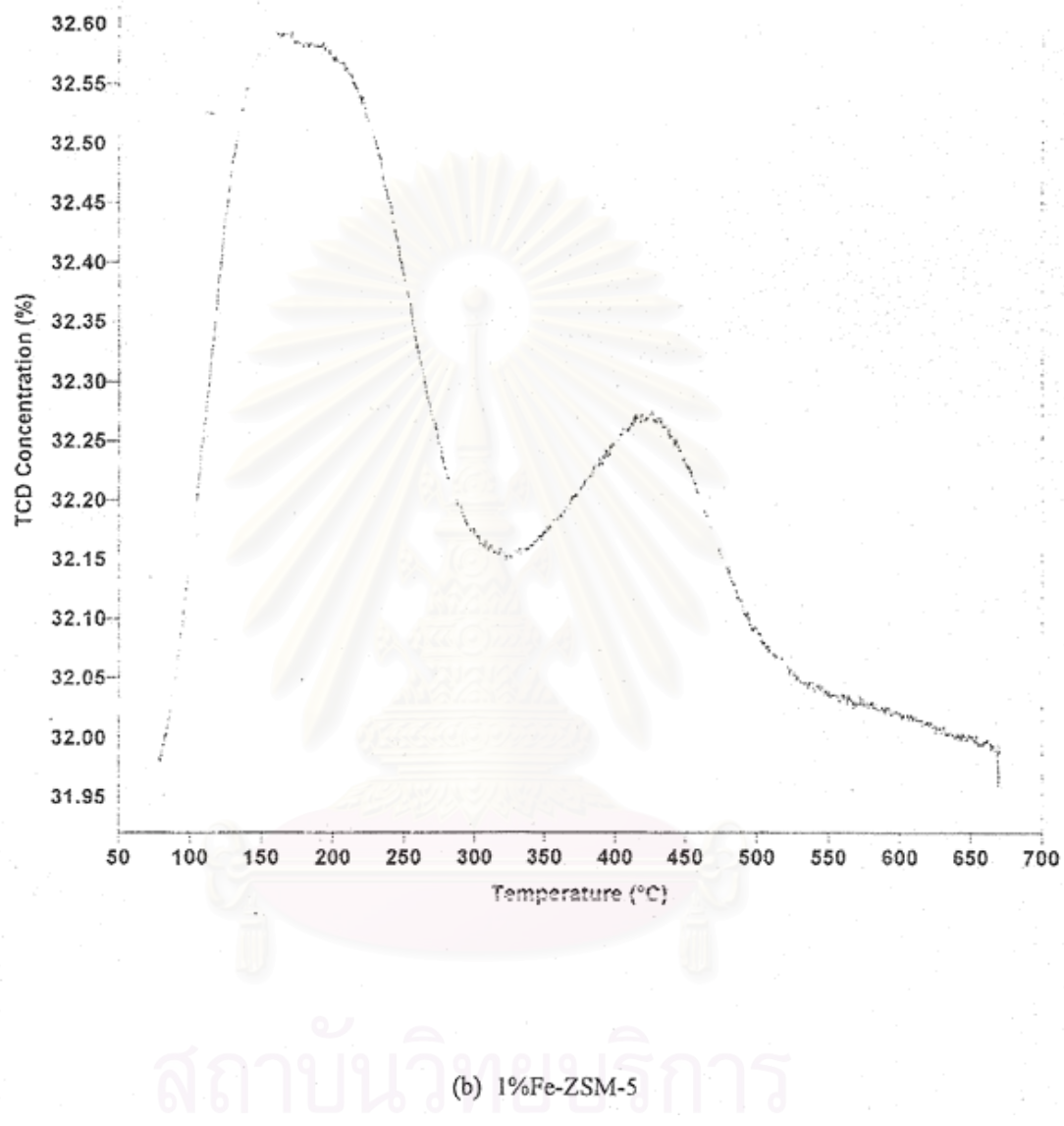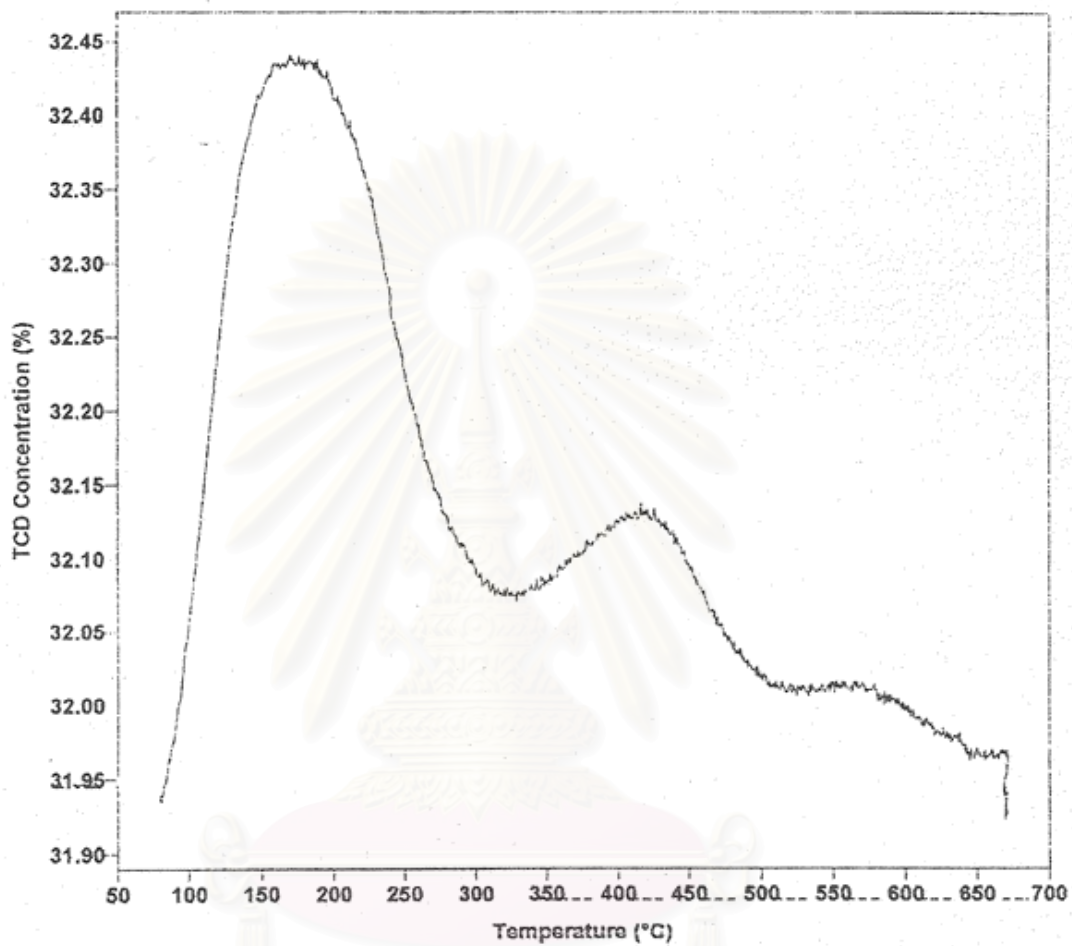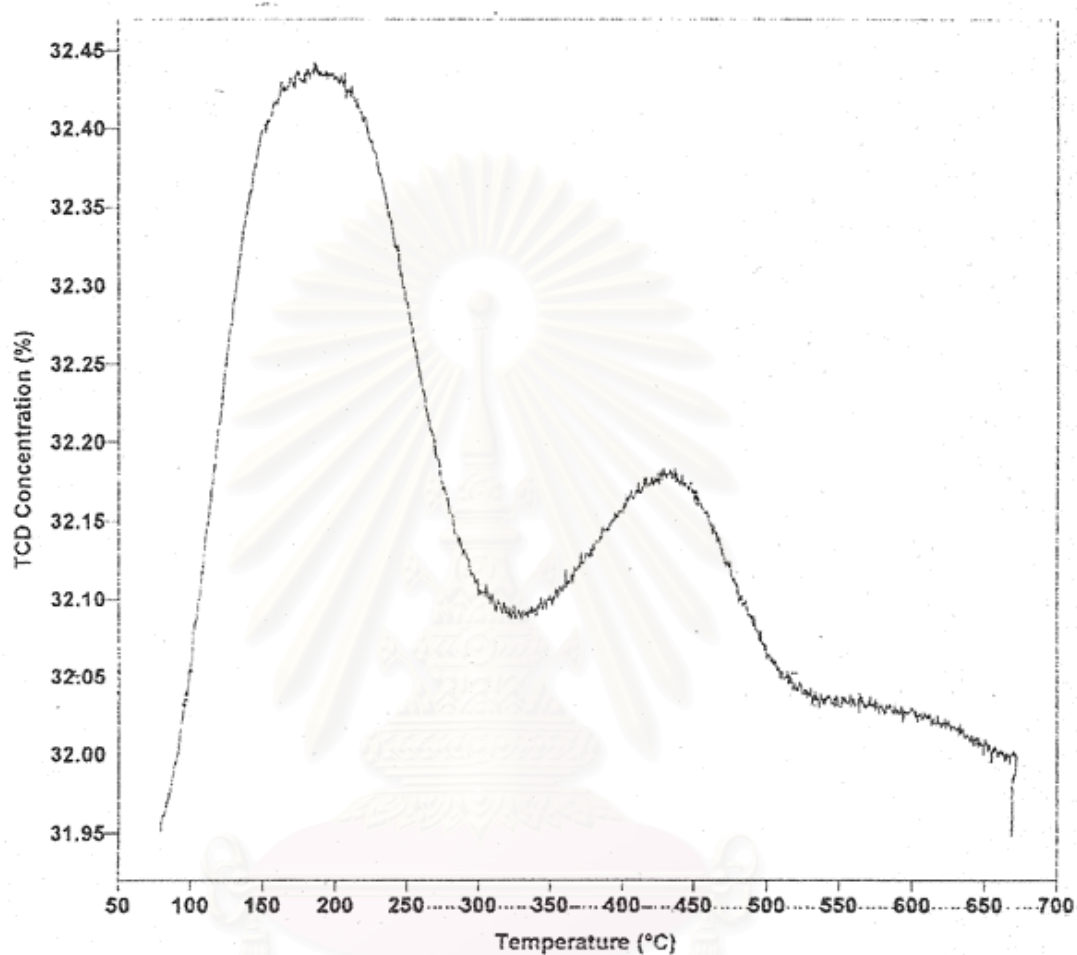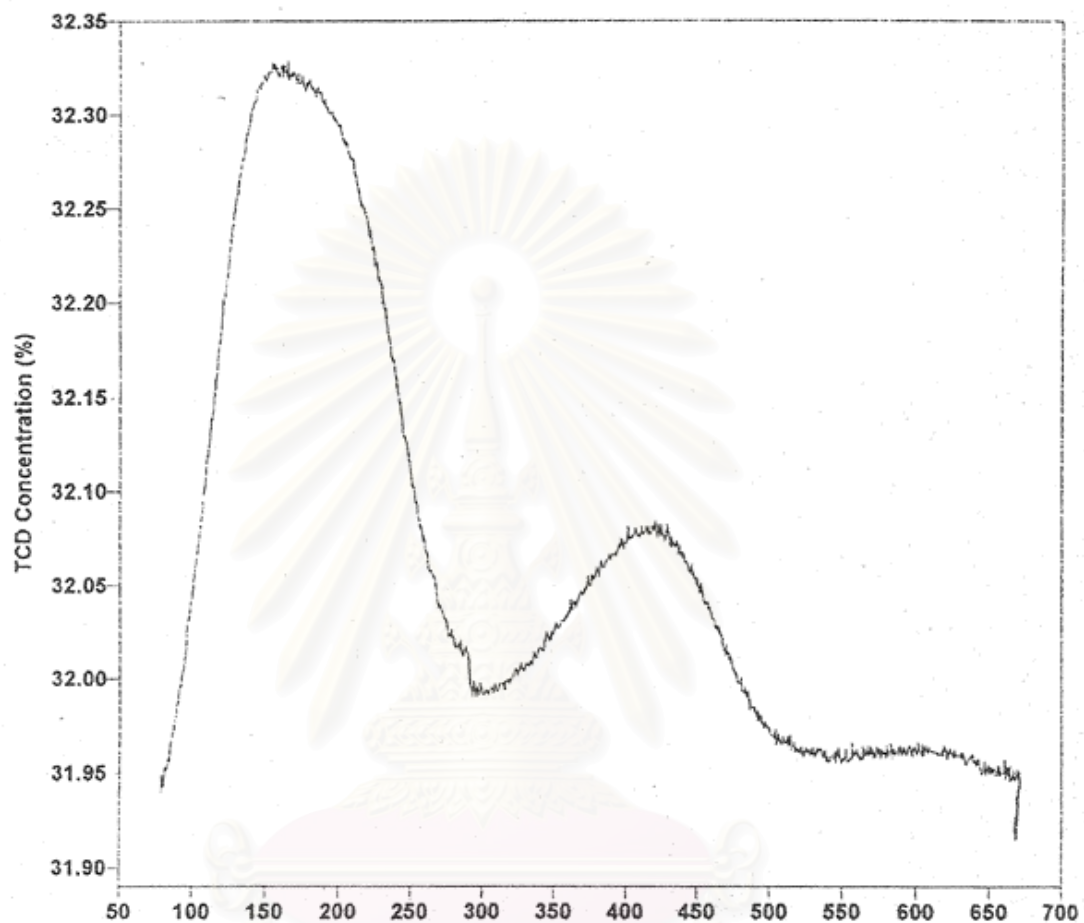
(e) 7%Fe-ZSM-5

Figure 5.3 The Temperature Programmed Desorption Profile
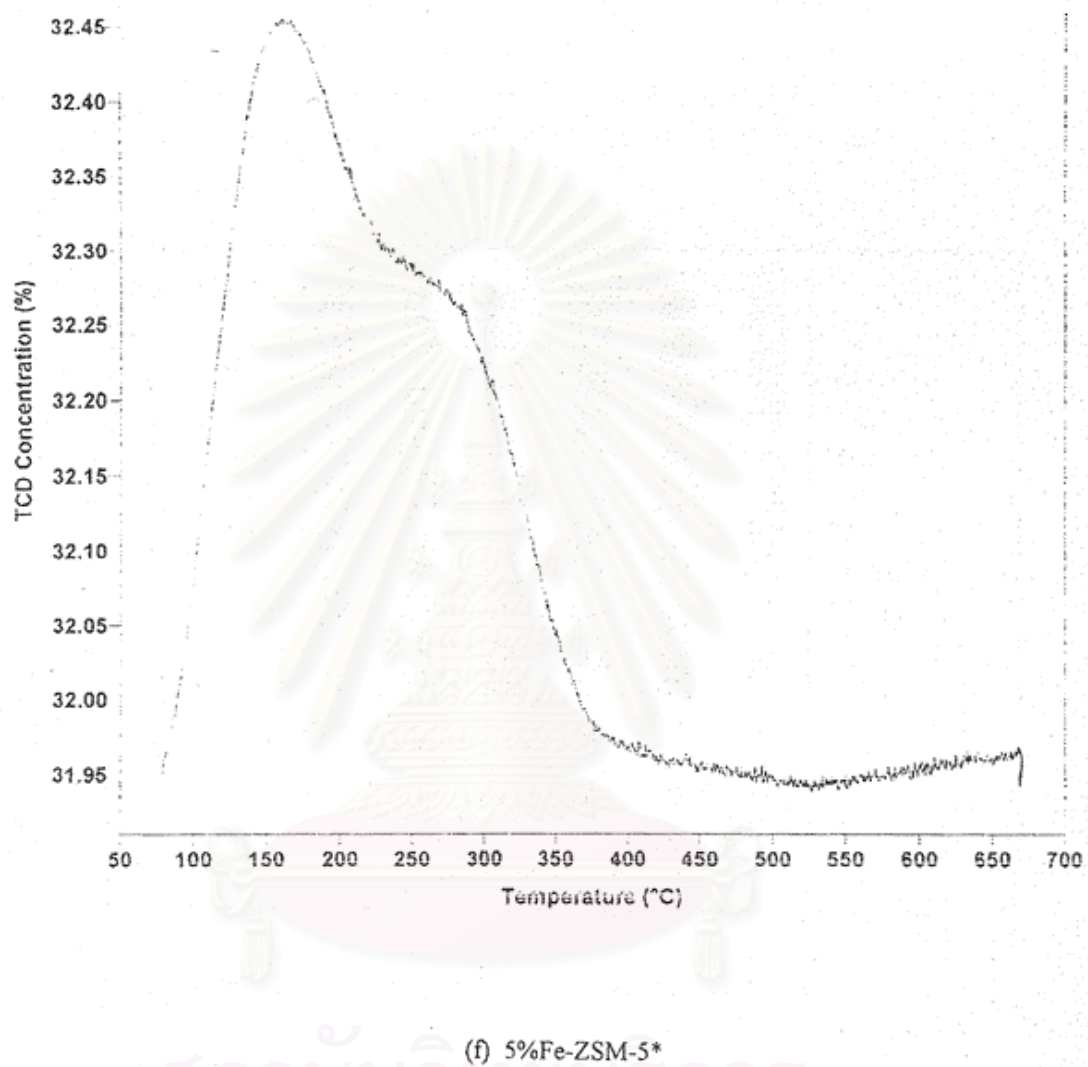
(f) 5%Fe-ZSM-5*

Figure 5.3 The Temperature Programmed Desorption Profile

5.2 Catalytic Reaction

In this section, the catalytic properties of the catalysts prepared in this reseach are investigated by testing the dehydration of ethanol (20Wt% ethanol).

5.2.1 The effect of catalysts on the dehydration of ethanol

The hydrocarbon distributions produced in different catalysts are shown in Table 5.5.

The reaction was carried out at the reaction temperature of 400 °C, GHSV of 2000 h^{-1}, 1 hour time on stream with the different catalysts
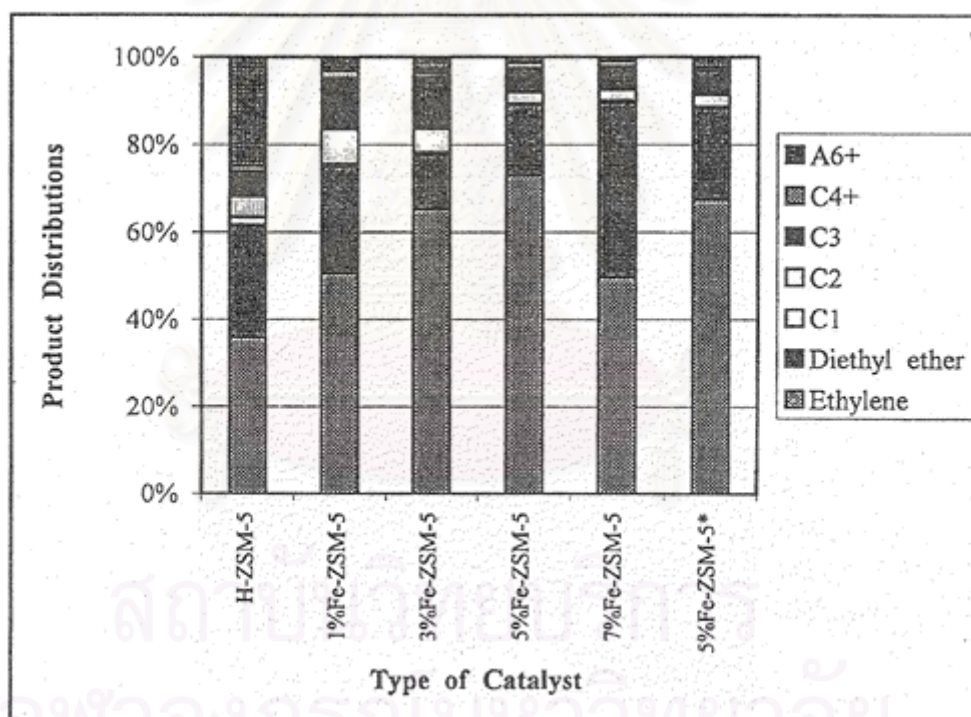

Figure 5.3 The effect of catalysts on the dehydration of ethanol.

Figure 5.3 shows the catalytic performance on dehydration of ethanol on ZSM-5 type catalyst. The selectivity for ethylene increased with the higher percentage of iron.

In this study, it can be seen that 5%Fe-ZSM-5 had the maximum selectivity of ethylene. Although 7%Fe-ZSM-5 had less strong acid sites than 5%Fe-ZSM-5 but zeolite structure had a significant effect on the catalytic performance. As the Figure 5.2, the structure of 5%Fe-ZSM-5 was better than 7%Fe-ZSM-5 and better than 5%Fe-ZSM-5 prepared by rapid crystallization, that effect the BET surface areas of 5%Fe-ZSM-5 was highest (Table 5.1).

5.2.2 The effect of reaction temperature on the dehydration of ethanol

The product distributions for 1 hour time on stream of ethanol dehydration at various temperature are shown in Figure 5.4

The reaction was carried out over 5%Fe-ZSM-5 was prepared by ion-exchange method at GHSV of 2000 h^{-1}
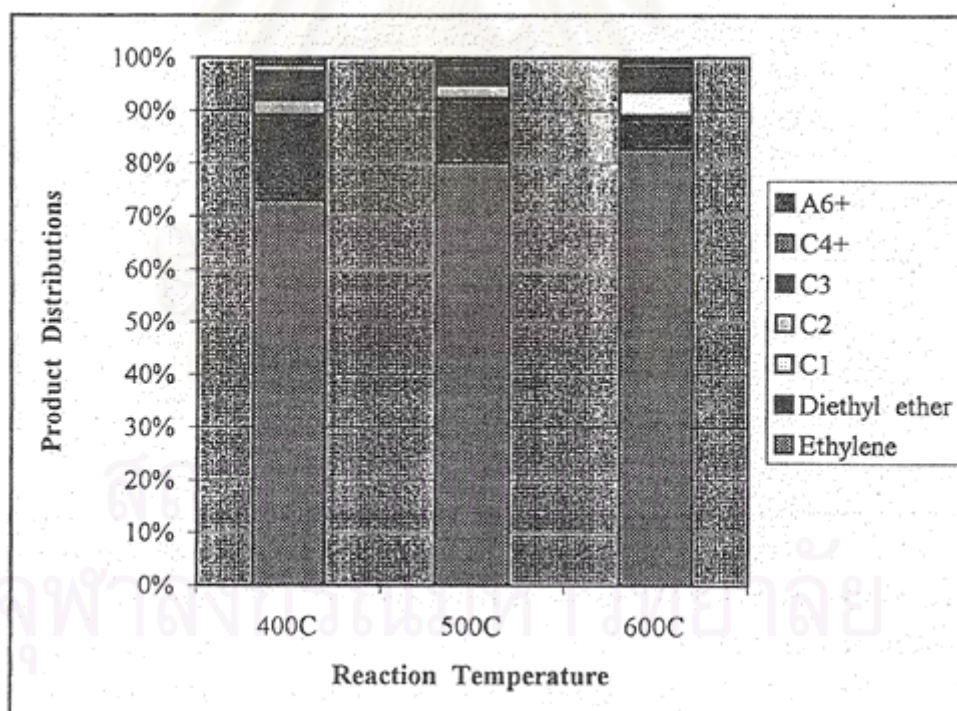

Figure 5.4 The effect of reaction temperature on the dehydration of ethanol.

From Figure 5.4, at high temperature (600°C), ethylene selectivity were higher than that of at low temperature (400,500 °C). That is, the ethylene selectivity increased when the reaction temperature increased.

5.2.3   The effect of GHSV on the dehydration of ethanol.

The product distributions for 1 hour time on stream at various GHSV are shown in Figure 5.5

The reaction was carried out over 5%Fe-ZSM-5 was prepared by ion-exchange method at reaction temperature of 600 °C.
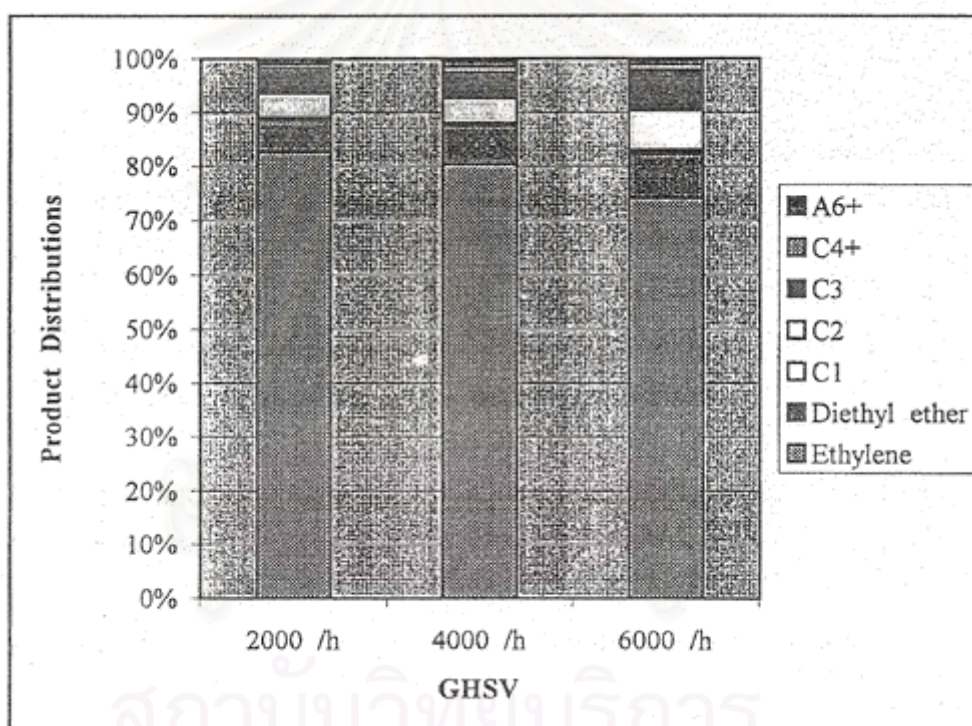
Figure 5.5 The effect of GHSV on the dehydration of ethanol

From Figure 5.5, the ethylene selectivity increased with decreasing space velocity. At GHSV of 2000 h^{-1}, a ethylene selectivity of 82.74% was achieved over 5%Fe-ZSM-5 prepared by ion-exchange method. Furthermore, the selectivity toward diethyl ether decreased with decreasing space velocity. This implies that diethyl ether was the initial product (intermediate) of the dehydration of ethanol and ethylene are formed by subsequent reaction of diethyl ether [Cory B., Ravindra (1997)].

CHAPTER VI
CONCLUSIONS AND RECOMMENDATIONS

6.1 Conclusions

The thesis dealt with studies on catalytic performance of ethanol dehydration to ethylene using H-ZSM-5 and Fe-modified ZSM-5 catalysts. The following conclusions of this study were drawn :

1. The 5%Fe-ZSM-5 catalyst prepared by ion-exchange had the best performance for dehydration of ethanol to ethylene that is ethylene selectivity (82.74%).

2. The optimum reaction condition for dehydration of ethanol to ethylene at atmospheric pressure was at temperature of 600 °C and GHSV of 2000 h^{-1}

3. The zeolite catalysts structure had a significant effect on the catalytic performance.

4. The BET surface areas of catalysts had a effect on the catalytic performance.

5. Fe modification contributed to the decrease in strong acid site.

6. The presence of Fe in ZSM-5 contributed significantly for higher ethylene selectivity than ZSM-5 without iron addition.

7. The ethylene formation not required strong acid sites.

8. Ethanol generated ethylene and diethyl ether. The formation of ethylene possibly proceeded via diethyl ether.

6.2 Recommendations

From this research, the recommendation for future study are as follows :

1. Study in more detail on state of Fe species in ZSM-5

2. Study in stability and life time of Fe-ZSM-5 catalyst.

3. Study the other transition metals to improve the ethylene selectivity.

REFERENCE

1. Cory B. phillips, Ravindra Datta, *Ind.Eng.Chem.Res.*, (1997), 36, 4466-4475

2. Raymond Le Van Mao, Thanh My Nguyen, *Applied Catalysis*, 48, (1989), 265-277

3. N. Srinivas, V.Radha Rani, S.J. Kulkarni, K.V. Raghavan, *Journal of Catalysis*, 208, 332-338, (2002)

4. Richard Joyner, Michael Stockenhuber, *J.Phys.Chem.B.*,(1999),103,5963-5976

5. S.P. Yuan, J.G. Wang, Y.W. Li, Haijun Jiao, *J.Phys.Chem.A.*, (2002), 106, 8167-8172

6. Kenneth F. Czaplewski, Thomas L. Reitz, Yoo Joong Kim, Randall Q.Snurr, *Microporous and Mesoporous Materials*, 56, (2002), 55-64

7. Vasant R. Choudhary, Suman K. Jana, Ajit S. Mamman, *Microporous and Mesoporous Materials*, 56, (2002), 65-71

8. P. Susavalli, *Production of ether from ethanol on catalyst,* A Thesis Submitted in Partial Fulfillment of The Requirements for the Degree of Master of Engineering, Department of Chemical Engineering, Chulalongkorn University, (1996)

9. Ashton, A.G., Batamanian, S. and Dwyer J., "Acid in Zeolite", *Catalysis by Acid-Bases*, Amsterdam: Elesvier, (1985)

10. Szoztak, R., *Molecular Sieve Principles of Synthesis and Identification*, 1-50, New York: Van Nostrand Reingold, (1989)

11. Tamake K.,Misona M.,Ona Y. and Hattori H., "New Solid Acids and Base", (Delmon, B. and Yates, J.T. *et.al.*), *Stud. Surf. Sci. Catal.*, 51, Tokyo: Elesvier,(1989)

12. Barthoment D., "Acidic Catalysts with Zeolites", *Zeolites Science and Technology*, Matinus Nijhoff Publishers, The Hemge, (1984)

13. Meier W.M., Olson D.H., "Atlan of Zeolite Structure Types", 3rd revised ed., *Int. Zeolite Assoc.*,Biston: Butter worth-Hoinemann, (1992)

14. Chen N.Y.,Garwood, W.E. Dwyer F.G., *Shape Selectivity Catalysis in Industrial Application*, 2[nd]ed. New York: Marcal Dekker, (1996)

15. Inui T.Yamase, O. Fugada K.,Itoh A. Tarmuto, J. Morina, Takegami Y., *Proceedings 8th International Congress on Catalysis*, Berlin, (1984), Vol.3, Dechema Frankfult-am-Main, (1984)

16. Meier, Olson, Baerlocher, *Atlas of Zeolite Structure Type*, (1996), 525

17. A. Kittivanichawat, *Conversion of Methane over ZSM-5 and Y Zeolites Containing a transition Metal.*, A Thesis Submitted in Partial Fulfillment of The Requirements for the Degree of Master of Engineering, Department of Chemical Engineering, Chulalongkorn University, (2001)

18. N. Oung, *Aromatic Synthesis from n-Heptane Using Modified MFI-Type Zeolite Catalyst.*, A Thesis Submitted in Partial Fulfillment of The Requirements for the Degree of Master of Engineering, Department of Chemical Engineering, Chulalongkorn University, (2000)

19. R. Le Van Mao, T.S. Le, M. Fairbairn, A. Muntasar, S.Xiao, G. Denes, *Applied Catalysis A: General*, 185, (1999), 41-52

20. Pál Fajes, János B. Nagy, János Halász, Albert Oszko, *Applied Catalysis A: General*, 175, (1998), 89-104

21. Kozo Tanabe, Wolfgang F. Hölderich, *Applied Catalysis A: General*, 181, (1999), 399-434

22. Yuguo Wang, Burtron H. Davis, *Applied Catalysis A: General*, 180, (1999), 277-285

23. I.P. Dzikh, J.M. Lopes, F. Lemos, F. Ramôa Ribeiro, *Applied Catalysis A: General*, 177, (1999), 245-255

24. Valyon J., Millman W.S., Hall W.K., *Cat. Lett.*, (1994), 24, 215

25. Feng X., Hall W.K., *J. Catal.*, (1997), 166, 368

26. Ramaswamy V., Gupta N.M., Chakrabaty D.K., *Catal.*, 12th, (1996), 95-99

27. Babu G.P., Hegde S.G., *J. Catal.*, (1983), 81, 471

28. Tsao. U., Reilly J., Dehydrate ethanol to ethylene, *Hydrocarbon Process*, (1978), 133-136

29. Jarvelin H., Koskinen M., Fray S.J., Refining processes, *Hydrocarbon Process*, (1996), 110-113

30. Winfield M.E., Catalysts, 7th ed, Reinhold Publishing Co., New York, (1960)

31. Chen N.Y., Making Gasoline by Fermentation, CHEMTECH, (1983), 488-489

APPENDICES

APPENDIX A
SAMPLE OF CALCULATIONS

A-1 Calculation of Si/Al Atomic Ratio for ZSM-5

The calculation is based on weight of Sodium Silicate ($Na_2O.SiO_2.H_2O$) in G2 and S2-solution.

M.W. of Si	=	28.0855
M.W. of SiO_2	=	60.0843
Weight percent of SiO_2 in sodium Silicate	=	28.5
M.W. of Al	=	26.9815
M.W. of $AlCl_3$	=	133.3405
Weigh percent purity of $AlCl_3$	=	97

For example, to prepare ZSM-5 at Si/Al atomic ratio of 20
Using Sodium Silicate 69 g with 45 g of water as G2-solution

$$\text{mole of Si used} = \frac{wt\,(\%)}{100} \times \frac{(M.W.\,Si)}{(M.W.\,SiO_2)} \times \frac{(1\,mole)}{(M.W.\,Si)}$$

$$= 69 \times \frac{28.5}{100} \times \frac{1}{60.0843}$$

$$= 0.3273$$

Si/Al atomic ratio = 20

Mole of $AlCl_3$ required	=	0.3273/20	=	0.0164 mole
Amount of $AlCl_3$	=	0.0164*133.34(100/97)		
	=	2.2496 g		

which used in G1, S1 solutions

A-2 Calculation of the amount of metal ion-exchanged ZSM-5

For example determine the amount of iron into catalyst = 0.2 wt%

The catalyst use = x g

So that

$$\frac{Fe}{(x + Fe)} = \frac{1}{100}$$

$$100*Fe = (1)(x+Fe)$$

$$(100-1)Fe = x$$

thus $$Fe = \frac{x}{(100-1)} \text{ g}$$

APPENDIX B
SAMPLE OF CALCULATIONS

Calculation of Gas Velocity

The catalyst used   = 0.2 g

Packed catalyst into quartz reactor (diameter = 0.6 cm)

Determine the average high of catalyst bed = x cm

So that, volume of catalyst bed = $\P*(0.30)^2*x$ ml-catalyst

Used GHSV (Gas Hour Space Velocity) = 2000 h$^-$

GHSV = volumetric flow rate/volume of catalyst = 2000 h^{-1}

Volumetric flow rate = 2000*volume of catalyst

$= 2000\P(0.3)^2x$ ml/h

$= 2000\P(0.3)^2X/60$ ml/min

at STP : volumetric flow rate   = [volume flow rate*(273.15+t)]/273.15

where t = room temperature, °C

APPENDIX C
DATA OF EXPERIMENT

Data for Figure 5.3 : Product distribution on dehydration of ethanol with different catalysts.

Catalyst	Product Distribution (Wt%)		
	Ethylene	Diethyl ether	Others
H-ZSM-5	35.88	35.70	28.42
1%Fe-ZSM-5	50.60	24.33	25.07
3%Fe-ZSM-5	65.20	12.46	22.34
5%Fe-ZSM-5	72.93	16.07	11.00
7%Fe-ZSM-5	49.71	39.89	10.40
5%Fe-ZSM-5*	67.32	21.08	11.60

*by rapid crystallization

Data for Figure 5.4 : The effect of reaction temperature on the dehydration of etyhanol

Reaction Temperature	Product Distribution (Wt%)		
	Ethylene	Diethyl ether	Others
400 °C	72.93	16.07	11.0
500 °C	80.02	12.12	7.86
600 °C	82.74	5.78	11.48

Data for Figure 5.5 : The effect of GHSV on the dehydration of etyhanol

GHSV	Product Distribution (Wt%)		
	Ethylene	Diethyl ether	Others
2000 h^{-1}	82.74	5.78	11.48
4000 h^{-1}	80.32	7.38	12.30
6000 h^{-1}	74.09	8.27	17.64

VITA

Miss. Unalome Wetwatana was born on February 19, 1978 in Bangkok, Thailand. She received the Bachelor's Degree of Science from the Department of Industrial Chemical, Faculty of Apply Science, King Mongkut's Institute of Technology North Bangkok (KMITNB) in 2000, She continued her Master's study at Chulalongkorn University in June, 2000